REVIEW SUMMARY

ADDITIVE MANUFACTURE

Material-structure-performance integrated laser-metal additive manufacturing

Dongdong Gu*, Xinyu Shi, Reinhart Poprawe, David L. Bourell, Rossitza Setchi, Jihong Zhu

BACKGROUND: Metallic components are the cornerstone of modern industries such as aviation, aerospace, automobile manufacturing, and energy production. The stringent requirements for high-performance metallic components impede the optimization of materials selection and manufacturing. Laser-based additive manufacturing (AM) is a key strategic technology for technological innovation and industrial sustainability. As the number of applications increases, so do the scientific and technological challenges. Because laser AM has domain-by-domain (e.g., point-by-point, line-by-line, and layer-by-layer) localized forming characteristics, the requisite for printing process and performance control encompasses more than six orders of magnitude, from the microstructure (nanometer- to micrometer-scale) to macroscale structure and performance of components (millimeter- to meter-scale). The traditional route of laser-metal AM follows a typical "series mode" from design to build, resulting in a cumbersome trial-and-error methodology that creates challenges for obtaining high-performance goals.

ADVANCES: We propose a holistic concept of material-structure-performance integrated additive manufacturing (MSPI-AM) to cope with the extensive challenges of AM. We define MSPI-AM as a one-step AM production of an integral metallic component by integrating multimaterial layout and innovative structures, with an aim to proactively achieve the designed high performance and multifunctionality. Driven by the performance or function to be realized, the MSPI-AM methodology enables the design of multiple materials, new structures, and corresponding printing processes in parallel and emphasizes their mutual compatibility, providing a systematic solution to the existing challenges for laser-metal AM. MSPI-AM is defined by two methodological ideas: "the right materials printed in the right positions" and "unique structures printed for unique functions." The increasingly creative methods for engineering both micro- and macrostructures within single printed components have led to the use of AM to produce more complicated structures with multimaterials. It is now feasible to design and print multimaterial components with spatially varying microstructures and properties (e.g., nanocomposites, in situ composites, and gradient materials), further enabling the integration of functional structures with electronics within the volume of a laser-printed monolithic part. These complicated structures (e.g., integral topology optimization structures, biomimetic structures learned from nature, and multiscale hierarchical lattice or cellular structures) have led to breakthroughs in both mechanical performance and physical/chemical functionality. Proactive realization of high performance and multifunctionality requires cross-scale coordination mechanisms (i.e., from the nano/microscale to the macroscale).

OUTLOOK: Our MSPI-AM continues to develop into a practical methodology that contributes to the high performance and multifunctionality goals of AM. Many opportunities exist to enhance MSPI-AM. MSPI-AM relies on a more digitized material and structure development and printing, which could be accomplished by considering different paradigms for AM materials discovery with the Materials Genome Initiative, standardization of formats for digitizing materials and structures to accelerate data aggregation, and a systematic printability database to enhance autonomous decision-making of printers. MSPI-oriented AM becomes more intelligent in processes and production, with the integration of intelligent detection, sensing and monitoring, big-data statistics and analytics, machine learning, and digital twins. MSPI-AM further calls for more hybrid approaches to yield the final high-performance/multifunctional achievements, with more versatile materials selection and more comprehensive integration of virtual manufacturing and real production to navigate more complex printing. We hope that MSPI-AM can become a key strategy for the sustainable development of AM technologies. ■

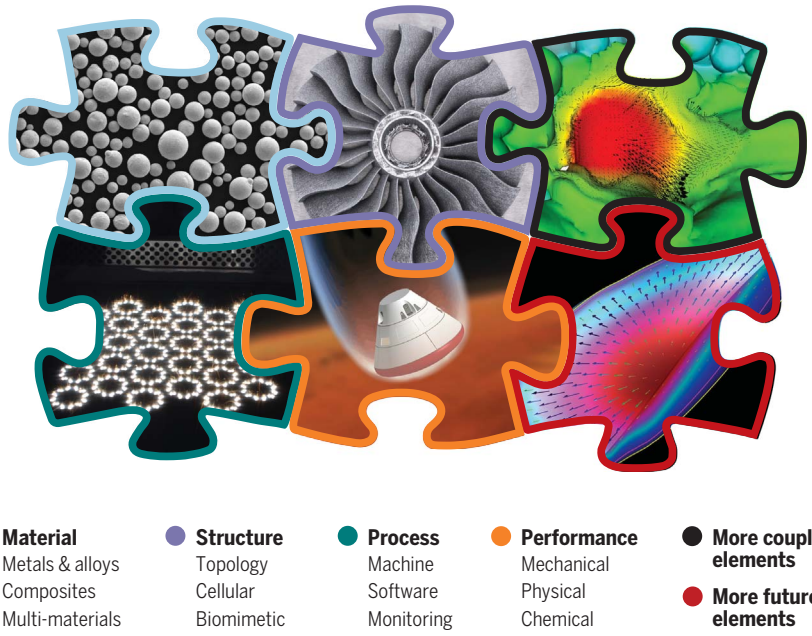

Material-structure-performance integrated additive manufacturing (MSPI-AM). Versatile designed materials and innovative structures are simultaneously printed within an integral metallic component to yield high performance and multifunctionality, integrating in parallel the core elements of material, structure, process, and performance and a large number of related coupling elements and future potential elements to enhance the multifunctionality of printed components and the maturity and sustainability of laser AM technologies.

The list of author affiliations is available in the full article online.
*Corresponding author. Email: dongdonggu@nuaa.edu.cn
Cite this article as D. Gu *et al.*, *Science* **372**, eabg1487 (2021). DOI: 10.1126/science.abg1487

READ THE FULL ARTICLE AT
https://doi.org/10.1126/science.abg1487

Downloaded from https://www.science.org on June 14, 2022

REVIEW

ADDITIVE MANUFACTURE

Material-structure-performance integrated laser-metal additive manufacturing

Dongdong Gu[1]*, Xinyu Shi[1], Reinhart Poprawe[2], David L. Bourell[3], Rossitza Setchi[4], Jihong Zhu[5]

Laser-metal additive manufacturing capabilities have advanced from single-material printing to multimaterial/multifunctional design and manufacturing. Material-structure-performance integrated additive manufacturing (MSPI-AM) represents a path toward the integral manufacturing of end-use components with innovative structures and multimaterial layouts to meet the increasing demand from industries such as aviation, aerospace, automobile manufacturing, and energy production. We highlight two methodological ideas for MSPI-AM—"the right materials printed in the right positions" and "unique structures printed for unique functions"—to realize major improvements in performance and function. We establish how cross-scale mechanisms to coordinate nano/microscale material development, mesoscale process monitoring, and macroscale structure and performance control can be used proactively to achieve high performance with multifunctionality. MSPI-AM exemplifies the revolution of design and manufacturing strategies for AM and its technological enhancement and sustainable development.

Metallic components are the cornerstone of modern industry (*1*, *2*). To a large extent, they also determine the service performance of an entire mechanical system. High-performance metallic components are typically applied in extremely severe environments. These components often have complex structures with various combinations of attributes such as ultralight weight, ultrahigh bearing capability, extreme heat resistance, and high reliability (*1*, *3*). Such combinations of attributes have major implications for material selection, manufacturing processes, and performance requirements. Laser-based additive manufacturing (AM), also known as 3D printing (3DP), is a key strategic technology for technological innovation and industrial sustainability (*4*, *5*). It allows for innovative design and integral manufacturing of end-use metallic components to meet the increasing demands of high-end industries (*6*, *7*).

At present, the two main representative categories for laser-based AM processes for metallic components are laser-directed energy deposition (LDED) and laser powder bed fusion (LPBF), according to the standard terminology for AM technologies established by the International Organization of Standardization (ISO)/American Society for Testing and Materials (ASTM) (*8*). Although LDED and LPBF share the same layer-by-layer fabrication methodology, they demonstrate distinctly different process procedures, material and laser parameters, and technological development directions and opportunities (*9*).

LDED is an AM process in which thermal energy (i.e., laser) is used to fuse materials (typically in the form of powder or wire) by melting as they are being deposited (Fig. 1A) (*8*). The thickness of deposited layers during LDED is typically no greater than 1 mm and may be as small as several hundred micrometers (*10*). A relatively large-sized laser beam, combined with a high laser power, is tailored to ensure both a high productivity and a sufficient laser energy input to melt the metals (Fig. 1B). One of the remarkable features of LDED is the high manufacturing speed with which it can be used to build large-scale components. Another feature of LDED is its high flexibility, extending its applicability from 3DP to surface coating (*11*), repairing (*12*), and remanufacturing (*13*). The precision of LDED metallic parts is relatively low, requiring subsequent machining to meet the designed structure and accuracy requirements.

LPBF is an AM process in which a laser, as focused thermal energy, selectively fuses regions of a powder bed (Fig. 1C) (*8*). The thickness of the deposited powder layer on the powder bed is typically below 100 μm (*10*), and accordingly the metallic powder for LPBF typically has a particle size one-third to one-half of that of powder for LDED. A successful LPBF depends on the uniform laying of powder layers, and therefore spherical powder particles with a high flowability are favored (*14*). Relative to LDED, LPBF uses a low laser power but a considerably finer laser beam with a high beam quality (Fig. 1D), which not only can carry sufficient laser energy to melt metals, but also can ensure a high printing accuracy. One of the important features of LPBF is its high manufacturing precision, making it suitable for the direct printing of complex structures. LPBF is typically applied for net-shaping small- and medium-sized components. As a result of high-speed scanner and multilaser scanning technologies, the forming size of LPBF is increasing and the maximum side length of build volume in the largest LPBF metal additive system today reaches 800 mm (*15*), making it possible to print components longer than 1 m.

Starting from the conceptualization of AM with single-material/simple-structure printing in the 1980s and 1990s, laser AM technologies developed rapidly in the 2000s and 2010s to produce complex metallic structures with improved mechanical properties (we call this "performance"). Laser AM increasingly emphasizes new materials and structures, as well as faster, bigger, and more unusual printing (*16*), introducing more physical and chemical properties and functionalities that were not possible previously (we term these "function") (Fig. 1E).

Although the industrial applications of laser-metal AM are continuously broadening, AM is still a developing technology by comparison to traditional casting, forging, and welding technologies. As a result, a series of scientific and technological challenges are emerging. First, the categories of commercially available metallic materials for AM are very limited. The process enhancement of AM urgently calls for serialization of existing and new materials with elevated AM applicability (*17*, *18*). Second, the point-by-point, line-by-line, and layer-by-layer localized forming characteristics of AM require cross-scale coordination across at least six orders of magnitude, including nano/microscale phase and microstructure control (material-related) (*19*, *20*), mesoscale interaction between laser and printing matter (process-related) (*21*, *22*), and macroscale component-forming processes, performance control, and application verification (structure- and performance-related) (*23*, *24*). However, as a consequence of the high complexity of the interaction of these multiple factors, the cross-scale control principles and methods for precise laser AM of metallic components have not been systematically established. Third, a successful laser-metal AM ultimately relies on performance enhancement or even multifunctional breakthrough of components. However, the material preparation, structure design, process control, and performance/function realization for laser AM are often empirical and are handled separately, and fundamental scientific theories that might guide a systematic approach are lacking. To tailor a complicated laser-metal AM for

[1]Jiangsu Provincial Engineering Laboratory for Laser Additive Manufacturing of High-Performance Metallic Components, College of Materials Science and Technology, Nanjing University of Aeronautics and Astronautics, Nanjing 210016, China. [2]Chair for Laser Technology LLT, RWTH Aachen/Fraunhofer Institute for Laser Technology ILT, D-52074 Aachen, Germany. [3]Laboratory for Freeform Fabrication, Mechanical Engineering Department, University of Texas, Austin, TX 78712, USA. [4]High-Value Manufacturing, School of Engineering, Cardiff University, Cardiff CF24 3AA, UK. [5]State IJR Center of Aerospace Design and Additive Manufacturing, School of Mechanical Engineering, Northwestern Polytechnical University, Xian 710072, China.
*Corresponding author. Email: dongdonggu@nuaa.edu.cn

Downloaded from https://www.science.org on June 14, 2022

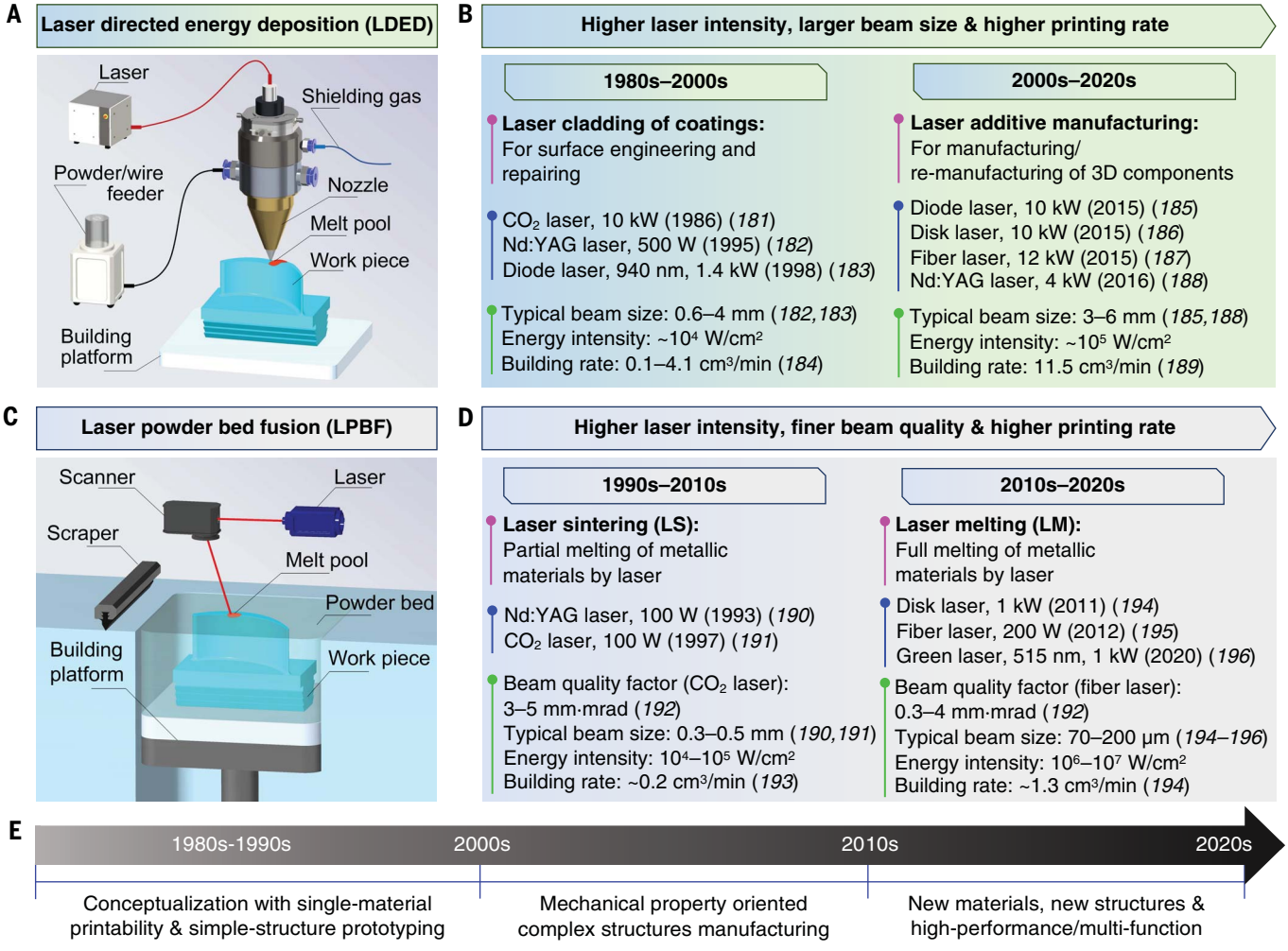

Fig. 1. Development of two categories of representative laser-metal AM technologies. (**A** and **C**) Schematics of LDED (A) and LPBF (C). (**B** and **D**) Typical development stages of processes (magenta-tagged), laser categories (blue-tagged), and laser and printing parameters (green-tagged) for LDED (B) and LPBF (D) of metals (*181*–*196*). (**E**) Timeline of major features and progress in the technological development of laser-metal AM.

a particular processing task therefore requires a complete, fundamental understanding of the basic sciences behind laser AM processes (*6*, *9*, *17*).

The interdisciplinary nature of laser-metal AM determines its rich scientific and technological connotations with respect to material (*25*–*28*), structure (*29*–*32*), process (*17*, *33*), performance/function (*34*–*36*), and associated applications (*37*–*39*). Several other excellent reviews address recent advances in these individual areas (*25*–*39*). We do not address these aspects separately, but instead propose a holistic concept of "material-structure-performance integrated additive manufacturing" (MSPI-AM) to cope with the extensive connotations of AM, providing a systematic solution to the above-mentioned challenges for laser-metal AM. We define the concept of MSPI-AM and highlight its characteristics, emphasizing opportunities for creating high-performance/multifunctional metallic components via MSPI-AM. We then propose cross-scale coordination mechanisms, basic sciences, and technical approaches for a proactive implementation of MSPI-AM. Finally, we share our perspective on future directions for the improvement of MSPI-AM and sustainable development of laser-metal AM technologies.

Defining MSPI-AM

Conventional design and manufacturing approaches for metallic components with multiple performance/function requirements usually involve the individual design of structures and materials and subsequent manufacturing and assembly. For example, in the aerospace industry, a planetary exploration lander is subject to an extremely severe service environment during landing (Fig. 2A), hence its bottom component has strict requirements for both mechanical and physical properties (Fig. 2, B and C). The commonly applied method for this category of components is hierarchical manufacturing and assembly, which involves several conventional methods such as equivalent manufacturing (e.g., forging, sheet metal forming, welding) and subtractive manufacturing (e.g., machining) (Fig. 2C). Equivalent manufacturing, exemplified by the bronze casting technique of early China, has more than 3000 years of development, whereas subtractive manufacturing technologies, promoted by the invention of electromotors, have emerged over the past 300 years (*40*). The equivalent and subtractive manufacturing processes have always proven to be irreplaceable to modern industries. Even so, the conventional route for the bottom component of the lander (Fig. 2C) normally requires repeated trial-and-error and coupling steps and, consequently, faces obstacles such as limited structure and material selection, complicated processes, serious overweight risk, and insufficient performance or function.

Laser AM has demonstrated substantial potential in high-performance/multifunctional design and integrated manufacturing of metallic components, turning "assembled parts" into an "integral component" (*29*, *30*). Currently,

Downloaded from https://www.science.org on June 14, 2022

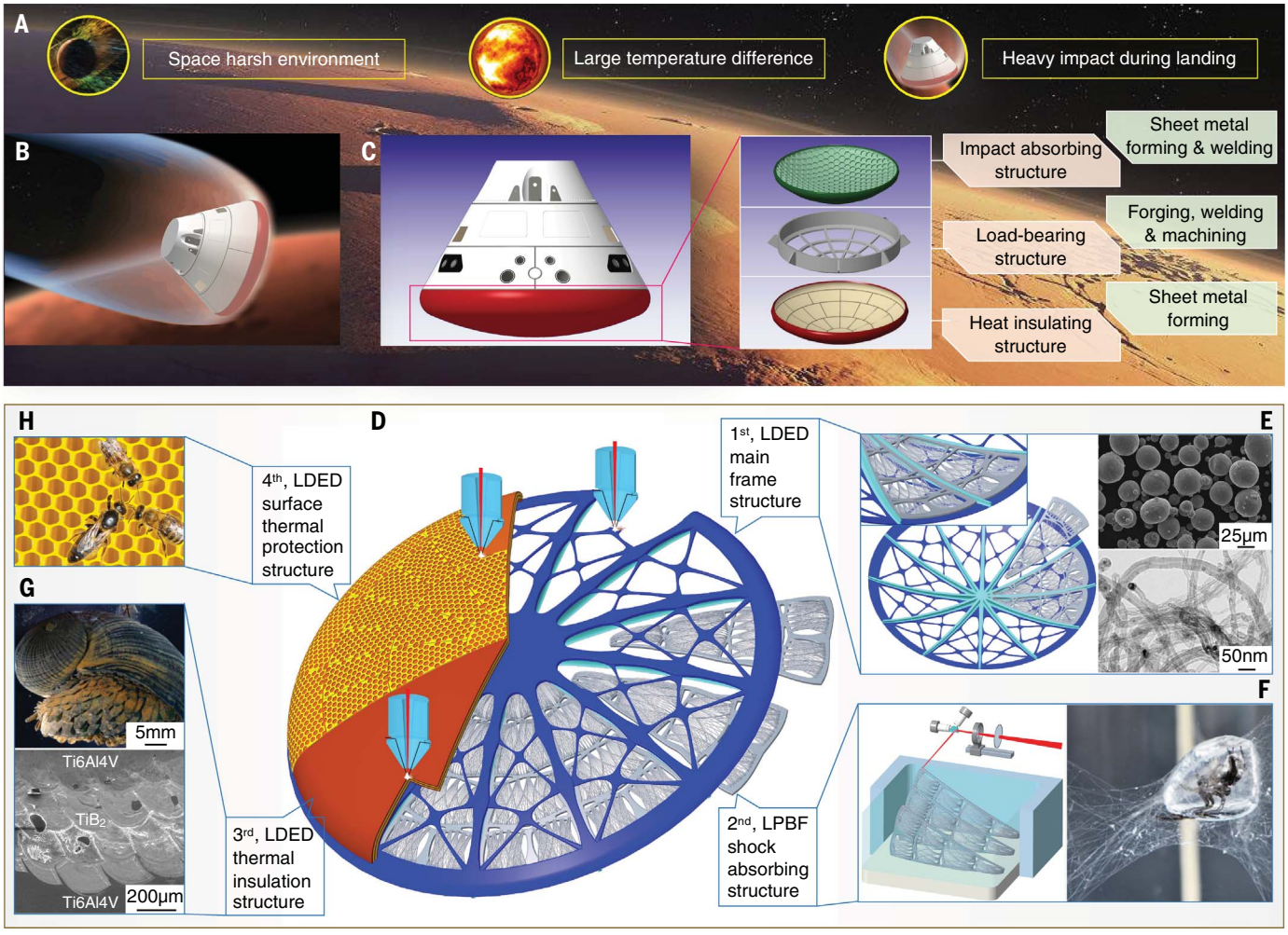

Fig. 2. Example of MSPI-AM of an integral metallic component for potential aerospace applications. (**A** and **B**) Schematics of a planetary exploration lander and an extremely severe service environment during landing. (**C**) Conventional hierarchical manufacturing and assembly approach for a bottom component of a lander with multifunctional requirements, likely to result in complicated processing procedures and overweight risk. (**D** to **H**) MSPI-AM approach for multifunctional design and manufacturing of an integral component. (D) Structure steps as described in Box 1. (E) LDED main frame structure, where carbon nanotube (CNT)–reinforced titanium-based nanocomposites are potential candidate materials (*80*). (F) LPBF shock-absorbing structure derived from the diving bell of a water spider [right image reproduced from (*197*) with permission]. The upper inset in (E) shows its assembly method along the stiffeners of the main frame structure. (G) LDED thermal insulation structure inspired by the natural armor of *Chrysomallon squamiferum* [upper image reproduced from (*198*) with permission], where multilayered Ti6Al4V/TiB_2 laminates are potential candidate materials (*199*). (H) LDED surface thermal protection structure derived from honeycomb (*200*).

material forming by AM enables high-performance printing of multimaterials such as metal-matrix composites (*41*–*43*), in situ composites or nanocomposites (*44*–*46*), and gradient materials (*25*, *47*, *48*). Structural innovations for AM, such as integrated topology structures (*49*, *50*), biomimetic structures (*51*, *52*), and hierarchical cellular or lattice structures (*53*, *54*), are emerging, leading to performance or function breakthroughs such as enhanced load bearing, energy/impact absorption, propulsion, and thermal management. Nonetheless, current laser-metal AM still follows a traditional route: A specific AM process, based on a particular structural design and material selection, is tailored to create components and ensure performance. This route is a typical "series mode"; "performance" occurs as the result of the printing ("process") of "material" and "structure." It may be necessary to adjust, respectively, the parameters in the domains of material, structure, and process to obtain the expected performance (*55*). This material-structure-process method—sequential but separately controlled—requires repeated trial and error to realize the performance of printed components (*56*).

MSPI-AM represents an opportunity to reduce this trial-and-error process. We define MSPI-AM as a one-step AM production of an integral metallic component by integrating multimaterial layouts and innovative structures, with an aim to proactively achieve the designed high performance and multifunctionality. With respect to multifunctionality, MacDonald and Wicker (*34*) have provided a state-of-the-art overview of multiprocess (or hybrid) 3DP, which entails not only the printing of multiple materials from metals to nonmetal materials but the embedding of active components to deliver electronic, electromagnetic, optical, chemical, and other functions (*34*). For 3DP of a metallic component, because of its high melting point and difficult-to-process nature, the material combinations and applicable AM processes have substantial limitations. The realization of multifunctionality of laser-printed metal components therefore becomes more difficult. Because the high-temperature printing of metals increases the difficulty of embedding active components and/or maintaining their functions (*57*), the multifunctionality of 3DP metallic components depends more on the design of multimaterials and novel structures.

Downloaded from https://www.science.org on June 14, 2022

Box 1. Example of MSPI-AM realization approaches and scientific issues.

We use the design and AM of a multifunctional integral bottom component for potential applications in the next-generation planetary exploration lander as an example to illustrate the concept of MSPI-AM, with its implementation philosophy, approaches, and scientific issues involved as follows. These scientific challenges and issues have common implications for laser AM of other similar materials and structures.

Integration of structures and materials: Performance-driven design of hierarchical structures and multiple materials

Hierarchical structure and function	Structural feature	Candidate materials	Scientific challenges and issues
(i) Lightweight, load-bearing main frame structure	Topology-optimized frame structure with stiffeners (Fig. 2E)	- High-strength Al alloy and Ti alloy - Al-matrix and Ti-matrix composites	- Laser printability and metallurgical defect control - Microstructure control and phase precipitation - Simultaneous enhancement of strength and ductility of printed materials
(ii) Shock-absorbing and impact-resistant structure	Reticular structure inspired by diving bell of water spider (Fig. 2F)	- High-strength Al alloy	- Response of materials to structural complexity and laser-forming ability - Relation between point-by-point printed material and overall structure performance
(iii) Thermal insulation structure	Multilayered structure inspired by natural armor of *Chrysomallon squamiferum* (Fig. 2G)	- Alloy/ceramic laminates - Alloy/alloy laminates	- Coordination of hardness, thermal conductivity, and coefficient of thermal expansion of materials - Control of interlayer printing defects and adhesion - Stress and deformation control of laser-printed integral curved surface
(iv) Surface heat–resistant and thermal protection structure	Cellular structure inspired by honeycomb (Fig. 2H)	- High-temperature Ti alloy - Ni-based superalloy	- Conformal deposition behavior and interfacial bonding properties of materials on curved surface - Microstructure and performance evolution of laser-printed materials at high temperature

Integration of processes: Multiprocess hybrid printing and integrated manufacturing

Printing and manufacturing procedures	Candidate processes	Scientific challenges and issues
Printing of main frame structure (i)	LDED with powder or wire	- Optimization of laser printing strategies and parameters for densification and defects control - Stress evolution and deformation control of main frame structure and stiffeners - Control and improvement of printing accuracy of topology optimization structures
Machining the assembly surface along stiffeners for structure (ii)	Computer numerical control (CNC) milling	
Printing of shock-absorbing structure (ii)	LPBF	- Coordination of laser powder-melting behavior and printing process - Control of metallurgical defects, e.g., balling effect, lack of fusion, porosity, and powder sticking - Dimensional accuracy and surface smoothness control of printed bioinspired reticular structures
Machining the assembly surface and assembling with structure (i) along stiffeners (Fig. 2E)	CNC milling and assembly	
Building the printing support for structure (iii) across surface of assembled structures (i) and (ii)	LDED	- Influencing mechanism of laser energy input on assembled structure and its deformation - Crack and deformation control of multimaterial laminated, curved surface structure - Interfacial interconnectivity of multimaterials and multistructures across different scales
Printing of thermal insulation structure (iii)	LDED	
Printing of thermal protection structure (iv)	LDED	- Interfacial adhesion of laser-printed high-melting-point material/structure on curved surface - Warpage and crack control of printed cellular structure under multiple structural and stress constraints

continued on next page

Downloaded from https://www.science.org on June 14, 2022

Integration of functions: Overall performance and function verification

Level	Testing and evaluation item	Scientific challenges and issues
Component level	Measurement of dimensional accuracy and detection of potential structural defects Tests on load-bearing, impact resistance, and heat protection/insulation properties Evaluating mutual interaction of various functions within an integral component	- Nondestructive testing methods for printing defects and structural integrity - Mapping relations of typical functions with structure, material, and process and related coordination mechanisms - Interfacial effect and coupling mechanism of multifunctions of laser-printed multistructures
System level	Systematic integration into a planetary lander and performance/function verification in a simulated real service environment	- Multifunction integration testing methods of complex integral component with multimaterials and multistructures - Multifunctional coupling and responsiveness of laser-printed integral component

The MSPI-AM strategy is therefore vital to the final high-performance/multifunctional goals of laser-metal AM.

MSPI-AM is within the framework of AM and inherits its enormous design freedom and other advantages. Also, MSPI-AM displays the revolution in design and available manufacturing strategies for AM, which elevates both the scientific challenges and technical approaches of AM. As an example, we apply MSPI-AM to the planetary lander example (Box 1). Versatile designed materials and innovative structures are simultaneously printed in different positions by multiprinters and multiprocesses within an integral component to yield a specific performance or function (Fig. 2, D to H). Use of the performance-driven MSPI-AM methodology leads to the design of multiple materials, new structures, and corresponding printing processes in parallel, with an emphasis on their mutual compatibility.

The right materials printed in the right positions

MSPI-oriented AM requires the controllable incorporation of multiple materials in different positions within a component to meet multiple requirements. Multiphase distribution with zero- to two-dimensional reinforcing phases is the simplest mode for multimaterial distribution in a microscale. The idea of alloying is normally realized by multiphase distribution and strengthening of 0D nanoparticles. Laser AM alloys—either conventional stainless steel (*58*) or recently developed Damascus-like maraging steel Fe19Ni5Ti (*59*) and high-strength Al-Mg-Sc-Zr (*60*), Al-Mg-Si-Sc-Zr (*61*), and Al-Mn-Sc (*62*) alloys—commonly demonstrate multiphase distribution with the precipitation of ultrafine nanoscale reinforcing particulates in specific positions of fused melt pools. LPBF processed alloys typically have heterogeneous hierarchical microstructures—consisting of fusion boundaries, dendritic and/or cellular structures, dislocations, precipitates, segregated elements, etc.—with the microstructural length scales spanning five to six orders of magnitude from nanometer to submillimeter (*58*, *59*). The solidification cellular structures are commonly reported in Fe-based and Al-based alloys produced by LPBF (*58*, *59*, *62*), which is a major contributor to the strength (*58*). The solute segregation and precipitates of nanoparticles are also observed along the walls of cellular structures in LPBF 316L stainless steel, which can promote dislocation pinning and twinning for a large uniform tensile elongation (*58*). Laser AM of alloys by adding secondary nanoparticles further highlights the precise design and control of multiphase distribution. A typical strategy is to introduce Zr nanoparticles as nucleants in 7075 aluminum alloy, which changes the columnar growth of dendrites to a fine equiaxed grain growth of matrix during LPBF, thus eliminating hot cracking by reducing solidification shrinkage and strain (*63*). Adding peritectic-forming lanthanum nanoparticles in titanium creates a promising laser solidification path for the α phase, yielding equiaxed microstructures with reduced anisotropy (*64*).

In contrast to the phase complexity of most alloys, high-entropy alloys (HEAs) have a high mixing configurational entropy originated from a mixing of five or more principal metal elements to stabilize the simple solid-solution structures (*65*, *66*). Both LPBF and LDED have demonstrated high potential in developing HEAs with excellent mechanical performance [e.g., strength-ductility synergy (*67*–*69*), fatigue (*70*), creep (*71*), and damage-tolerant (*72*) behaviors] and functions [e.g., magnetic property (*68*), corrosion resistance (*69*, *72*), and high-temperature oxidation resistance (*73*)]. Laser-induced superfast cooling rates of LDED and LPBF help to prevent the formation of detrimental intermetallic compounds and the diffusion of constituent elements (*65*). However, laser rapid solidification tends to cause a large temperature gradient and resultant residual stresses, intensifying the possibility of cracking in laser-printed HEAs. The element combinations free of formation of intermetallics and insensitive to stress and cracking are recommended primarily for the composition design of HEAs to enhance their laser printability (*65*). Another advantage of LDED and LPBF for HEAs lies in their capability to yield a hierarchy of microstructures including grain refinement, elemental segregation and precipitation, increased dislocation density, and deformation twinning (*66*, *74*), thereby facilitating the microstructural and performance/function manipulation of laser-printed HEAs.

The formation of composites by incorporating different metal matrices and reinforcing phases can make the types, contents, morphologies, and distributions of reinforcements more diverse and designable. A homogeneous incorporation of ceramic particles throughout a matrix is the most common layout manner for reinforcement (*75*) (Fig. 3A). Unfortunately, the easily occurring particle agglomeration and limited ceramic-metal wettability cause interfacial micropores and cracks, as well as a dilemma known as strength-ductility trade-off (*76*). Interface modification through laser-tailored construction of a gradient interfacial layer between ceramic and metal proves efficient in eliminating interface defects and achieving a simultaneous improvement of strength and ductility (*77*–*79*). Laser-tailored in situ reaction further expands the formation mechanisms of reinforcing phases. Laser-metal AM is distinguished by its unique laser energy feature and metallurgical mechanism. The peak temperature in laser-induced melt pool can be several hundred degrees above the liquidus temperature of an alloy, and even as high as the boiling point of the alloy for keyhole mode printing (*17*). The cooling rates during laser rapid solidification reach 10^5 to 10^7 K/s for LPBF and 10^2 to 10^4 K/s for LDED (*6*, *9*). Laser-tailored in situ reinforcements can have novel 1D whisker- or strip-structured (*80*) or 2D nanosheet- or lamellar-structured (*81*) growth features (Fig. 3, B and C) with metallurgically coherent interface with the matrix. The synergistic action of novel reinforcing structure, interfacial coherence, and matrix microstructures/dislocations contributes substantially to the enhancement of both mechanical performance [e.g., tensile (*41*–*43*), wear/friction (*82*, *83*)] and physical or chemical

Downloaded from https://www.science.org on June 14, 2022

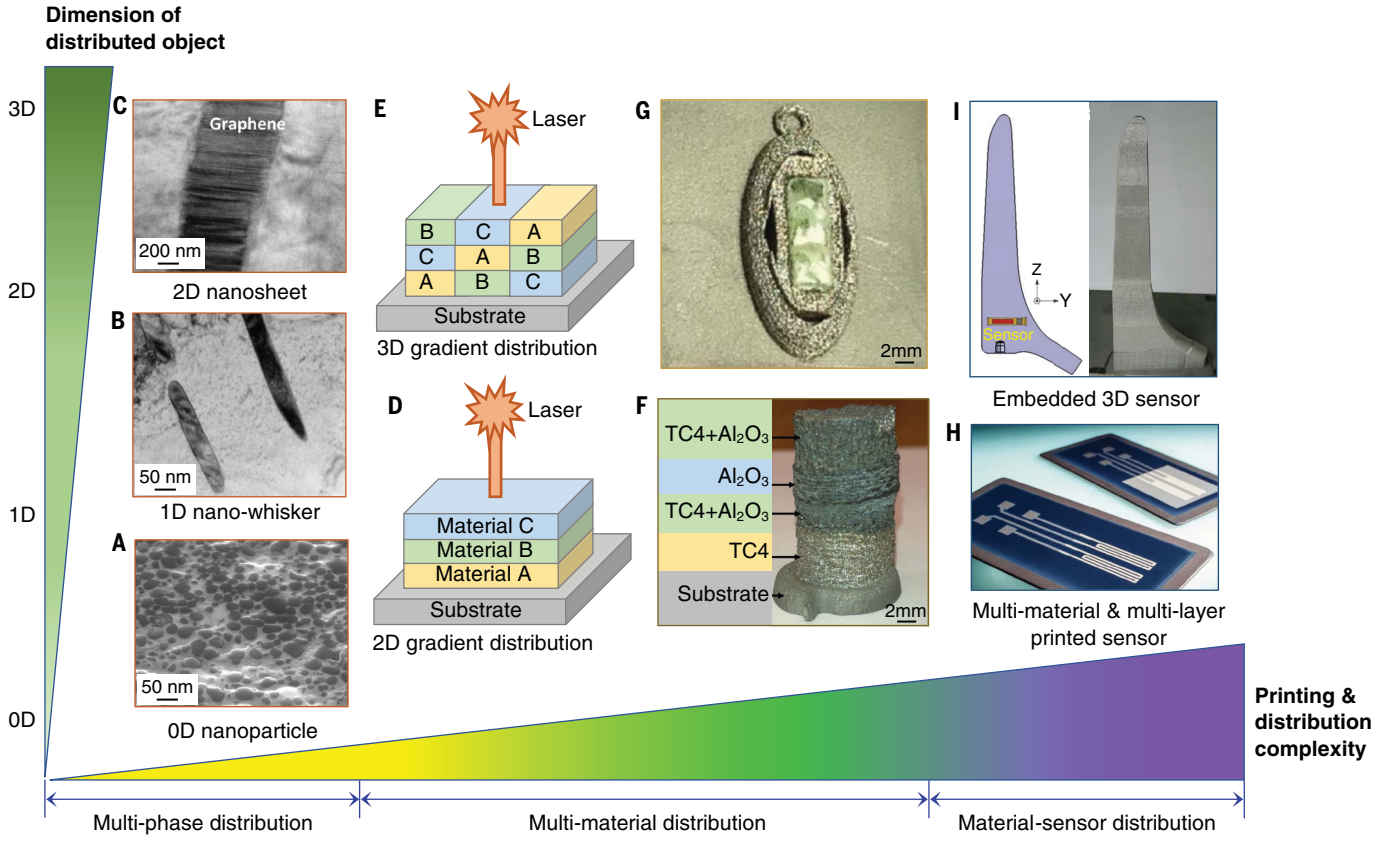

Fig. 3. Laser AM of multiple materials and sensors within a monolithic metallic component to demonstrate "the right materials printed in the right positions." (**A** to **C**) Multiphase distributions in laser-printed metal-matrix nanocomposites: (A) zero-dimensional (0D) TiC nanoparticles in Al matrix [image reproduced from (*75*) with permission], (B) one-dimensional (1D) nano-whisker structured TiC reinforcement in Ti matrix (*80*), and (C) two-dimensional (2D) graphene nanosheet in Fe matrix [image reproduced from (*81*) with permission]. (**D** to **G**) Multimaterial distributions in laser-printed compositionally graded structures. [(D) and (F)] LDED Ti6Al4V (TC4)–Al_2O_3 multimaterial structure with 2D gradient distribution of different materials between deposited layers [(F); image reproduced from (*89*) with permission]. [(E) and (G)] LPBF 316L–glass multimaterial object with 3D gradient distribution of different materials both within and between deposited layers [(G); image reproduced from (*90*) with permission]. (**H** and **I**) LPBF enabling the structural integration of sensors in complex monolithic metallic structures. (H) Selective laser-sintered temperature sensor structures on a glass insulation layer (blue) and on a stainless steel substrate (gray) [image reproduced from (*103*) with permission]. (I) Selective laser-melted smart femoral hip stem with the embedded sensor in the printed carrier structure [image reproduced from (*104*) with permission].

functions [e.g., high-temperature oxidation resistance (*84*, *85*), corrosion resistance (*86*, *87*), superhydrophobicity (*88*)] of laser AM components.

Nozzle-based LDED is sufficiently flexible to enable a macroscale layout of two or more materials within a single component. With multiple powder or wire feeders, this approach allows for the depositing of multiple materials in various positions to yield compositionally or functionally graded structures by dynamically changing the desired materials at specific times and positions during printing. One of the most widely applied forms for multimaterial printing is the 2D gradient distribution of different layers of materials along a building direction (*25*, *47*, *89*) (Fig. 3, D and F). The 3D gradient distribution of different materials both within and between deposited layers, despite its higher technical difficulty, offers a more site-sensitive and material-specific mode for multimaterial layout (Fig. 3E). With the development of an in situ powder mixing and feeding system in a LPBF machine, the LPBF process, which was previously limited to single-material use (*25*), broadens its capability in multimaterial printing (Fig. 3G) (*90*, *91*). A great challenge for AM quality control is miscibility of the deposited material layer with the previously deposited ones (*92*). Mismatches in physical properties (e.g., melting temperature, laser absorptivity, coefficient of thermal expansion, and thermal conductivity) are the governing factors in inhibiting intermaterial/interlayer bonding (*25*, *47*, *92*).

The first step toward reducing the degree of mismatch is to optimize multimaterial combination. Metal-metal combinations [e.g., stainless steel 316/316L with Ti-6Al-4V (*93*), Inconel 625 (*94*), and copper alloys (*91*, *95*)] demonstrate the processability required to achieve gradient structures using both LDED and LPBF. Nonetheless, the formation of brittle intermetallic phases is prone to occur at the gradient interface, which is a main cause for cracking and even delamination of deposited materials (*92*–*94*). A direct metal-ceramic AM in a single component is still far from mature (*25*). In some extreme cases, the temperature at which a ceramic can efficiently melt and flow is even higher than the vaporization temperature of a metal. Altering printing parameters and strategies according to the specific materials being printed is the second measure to create a targeted printing environment to alleviate the detrimental influence of material mismatch (*89*, *91*, *93*, *96*). Third, the compositional gradation approach, which introduces a gradual transition structure between ceramic and metal, is efficient in reducing mismatch and metallurgical defects. It can be a compositional intermediate layer designed in the component model to metallurgically

Downloaded from https://www.science.org on June 14, 2022

bond two immiscible materials during AM (*97*). Another ingenious transformation is the printing of ceramics in the form of metal matrix composites (MMCs) (*98*, *99*) to increase compatibility with metals. The contents of ceramics can continuously change in gradient along one or more spatial directions to allow for the local tailoring of properties.

Beyond the alloys, composites, and multimaterials with spatially varying microstructures and properties, the next level of complexity of 3DP is the integration of functional structures with electronics within the volume of a printed part (*34*, *57*, *100*, *101*). This "material-sensor" distribution, with structural integration of active components in a laser-printed monolithic part, delivers more functionality and even intelligence, thereby broadening the connotation of "multimaterial" printing. 3DP structures with electronics have comprehensive requirements of high surface finish and minimal porosity, high structural precision and spatial resolution, and superior electrical, thermal, and mechanical properties (*102*). A multiprocess production combining AM and complementary processes is necessary to realize material-sensor distribution, providing spatial control of the main structure, active components, subcomponents (e.g., wires and antennas), and available functionality. First, the integration of sensors into a customized component can be realized by either (i) multilayer AM of different materials to build up an entire, individualized sensor compatible with a structure without adhesives (*103*) (Fig. 3H) or (ii) embedding of sensors directly into a printed structure with AM process interruption, followed by the creation of connections between sensors and surrounding components to obtain sensitivity (*104*) (Fig. 3I). For this purpose, a multiprocess AM production route should be optimized to avoid the detrimental influence of the surrounding printing matter (e.g., possible residual metal powder) on the functional efficiency of encapsulated active components (*105*). Second, the operative temperature of laser-metal printing should be strictly controlled to avoid overheating and maintain the functions of temperature-sensitive active components (*57*). Third, the installation position and functional connection interfaces of active components need to be designed to achieve a balance between the laser printability of basic structures and the operability of the embedding process (*104*–*106*).

Unique structures printed for unique functions

"Design for AM" has received intensive attention as a means of broadening the freedoms and benefits of AM technologies (*29*, *30*). Design for AM integrates multiscale levels, ranging from material-level design with microstructural complexity to component-level design with macrostructural complexity. We use three representative structures for AM—topology structure, cellular structure, and biomimetic structure—to describe the methodologies, principles, challenges, and solutions for structural design and multifunctionality for laser-metal AM (Fig. 4) that are also broadly applicable to other materials and structures.

Topology optimization (TO) design of monolithic components is of particular importance for applications of AM in building aircraft, aerospace, and automotive structures (*32*, *50*), primarily motivated by the substantial weight reduction (*29*–*32*). For example, a satellite bracket with TO configuration filled with internal lattice structure results in a 17% weight reduction (Fig. 4A) (*50*). The AM-applied TO is often in the structural domain (*29*). The structural TO determines the optimal layout of the solid or void of subregions that constitute a continuum structure (*107*) in order to achieve a desired performance or functionality for a given set of loads and constraints (*29*, *108*). Structural TO assumes that the structure is composed of a single homogeneous material and that material is either present or absent in each subregion of the design domain (*29*, *107*). The best distribution of material is realized by creating, merging, and splitting interior voids during structural evolution (*31*). Therefore, the essence of TO is to place the voids and materials of appropriate sizes and configurations into the appropriate positions of a monolithic component, reaching its design goals such as minimal material usage, uniform stress distribution, and long service life. As AM substantially increases design freedoms by reducing some manufacturing limitations, AM-assisted TO has advanced from the preliminary weight-saving structural design of a single homogeneous material to complex multimaterials and multiphysics design (*109*). Many examples are available where laser-based metallic AM is making a substantial impact on the promotion of TO to a multifunctional level (*110*–*113*). TO has been applied in a range of design objectives for AM to fulfill multifunctionality [e.g., heat conduction (*110*) and thermal-fluid (*111*), electromagnetic (*112*), and shockwave propagation (*113*)].

This sort of TO design brings merit to an application only when it has manufacturability. Although a majority of TO structures could be printed by polymer-based AM processes, difficulties may arise when using metallic AM for the direct printing of nontailored TO structures (*30*), especially when handling the multimaterial, multiphysics, and multifunctional TO. Laser-metal AM introduces extra manufacturability-related constraints or boundary conditions to TO, such as supports for overhanging structures, minimum printable structural resolution, anisotropic material properties, and interior strain and stress (*30*, *32*). Research on TO for AM should be accordingly geared toward both physically and digitally print-ready TO designs (e.g., support-free structures, smooth and well-defined boundaries, etc.) in order to bridge the challenges of TO design and laser-metal AM fabrication (*32*).

Cellular structures (CSs) are another category promoted by AM. CSs are created by designing the configuration and volume fraction of a unit cell having a characteristic scale of 0.1 to 10 mm (*53*), building up a volume based on an interconnected network of unit cells. Foams (random connectivity of unit cells), lattices (regular/periodic connectivity), honeycombs, and structures similar to these are included in CSs (*53*). From the primary target of lightweight CSs produced by AM, the minimum wall thickness and finest resolvable feature size are the manufacturing constraints (*29*, *32*). Therefore, the basic idea of material distribution for CSs is to put the minimum amount of materials only where it is necessary for particular functions and applications. Laser AM can create hard-to-produce metallic CSs with specific mechanical, thermal, acoustic, optical, and biological properties (*29*). Typically, the mechanical behavior of CSs is anisotropic (*53*), and the type, dimension, orientation, and boundary conditions of the periodic unit cells determine the final porosity, properties, service, and failure mechanisms. Various optimization methods [e.g., computer-aided design and finite element modeling (*53*) and topology optimization (*29*)] are developed for the design of CSs, particularly considering the periodicity of unit cells, homogenization of interconnected networks, and additive manufacturability. Although periodic arrangements of identical unit cells are common for a vast majority of CSs, a conceptual change in printing multiscale, hierarchical lattices by mimicking crystalline microstructures (Fig. 4B) yields robust and damage-tolerant functions relative to arrangements of identical unit cells (*114*), which opens up opportunities for architected CSs with breakthroughs in functionality. This lightweight and damage-tolerant architected structure has potential applications in producing the blades for next-generation airplane engine (*114*) where each blade contains multiple cellular domains that are filled with crystal-inspired meso-lattice features (Fig. 4B).

After 3.8 billion years of natural evolution, organisms have optimized complex materials and structures to fulfill specific functions to meet the competition from the external environment (*115*). "Biomimicry" or "bioinspiration," the development of solutions based on biological adaptations, aims to provide the optimized material and structural strategies learned from nature in solving engineering problems (*51*, *52*). An example of the magic of bioinspiration is the full-scale aircraft wing optimized by gigavoxel computation and 3DP-demonstration, which shows remarkable

Downloaded from https://www.science.org on June 14, 2022

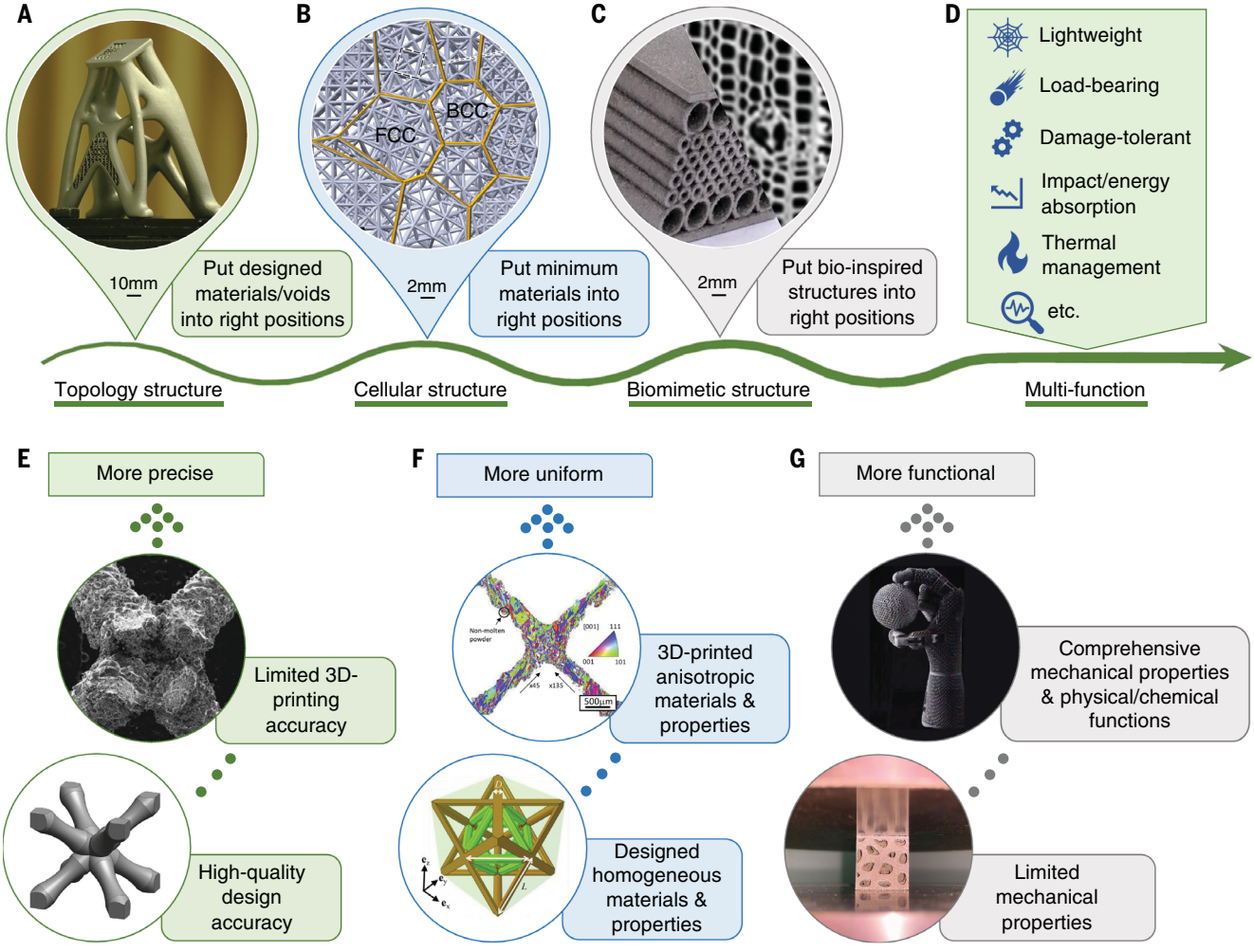

Fig. 4. Multifunctional laser-metal AM through structural design and innovation to reflect the idea of "unique structures printed for unique functions." (**A** to **D**) Three representative innovative structures for AM and attendant multifunction, including (A) a topology-optimized satellite bracket filled with lattices [image reproduced from (*50*) with permission], (B) a crystal-inspired cellular structure containing hierarchical face-centered cubic (FCC) and body-centered cubic (BCC) lattices [image reproduced from (*114*) with permission], and (C) a functional graded sandwich structure inspired by the Norway spruce stem (*118*, *119*). (**E** to **G**) Three categories of existing gaps and development directions in multifunctional laser-metal AM, in terms of (E) manufacturing accuracy [upper image reproduced from (*122*) with permission; lower image reproduced from (*121*) with permission], (F) material and property anisotropy [images reproduced from (*123*) with permission], and (G) diversity of functions [upper image reproduced from (*34*) with permission].

similarity to naturally occurring bone structures of bird beaks (*116*). A general methodology for biomimetic AM consists of problem definition, analogy search and preselection, analysis and abstraction of biological model, and transfer to engineering design and AM production (*117*). Biomimetic AM implies the bioinspired printing of naturally optimized structures to yield multifunctional components. A key challenge is how to "duplicate" the finely developed natural structures with the right materials. An example is the selective laser-melted lightweight, functional graded sandwich structure inspired by the Norway spruce stem and printed with titanium alloy, having both thermal protection (*118*) and load-bearing (*119*) functions, which finds its potential applications in the aerospace industry for components of hypersonic vehicles and reusable launch vehicles (*118*) (Fig. 4C).

The use of digital imaging tools (e.g., x-ray microcomputed tomography) (*115*) can yield an in-depth understanding of natural structures, which is particularly important for determining spatial structural and material information as bioinspiration for AM design. Bioinspired structural design elements typically have eight common categories of fibrous, helical, gradient, layered, tubular, cellular, suture, and overlapping structures (*120*). A true natural structure, however, exhibits the multiscale hierarchical repetition of various structural forms to provide superior properties over a single structure. Meanwhile, material multiplicity and their layout manner contribute to the particularity of natural structures. Although their compositions are considerably different from those of metals, the material layout principles are worth learning and implementing in high-performance/multifunctional AM design and production.

The various forms of material and structural complexities bring substantial challenges to AM manufacturability. The first challenge is the gap between the designed high-quality surface and structural precision and the limited manufacturing accuracy and quality (*121*, *122*) (Fig. 4E), caused by some typical defects associated with laser-metal AM such as (i) sticking of unmelted powder, balling effect of melt and rough surfaces (*53*); (ii) residual microporosity and metallurgical imperfections (*115*); and (iii) residual stresses and resultant deformation and cracking (*117*). The efficient control of these defects toward a higher printing precision

Downloaded from https://www.science.org on June 14, 2022

depends on the tailored coordination of a whole printing chain including laser-material absorption, material melting, formation of melt pool, and subsequent rapid solidification. The second challenge is the anisotropy of materials and properties (*123*) (Fig. 4F), which is either the process-induced anisotropy caused by the layer-by-layer manufacturing nature of AM or the intrinsic anisotropy arising from the material or structure itself (e.g., multilayered composites or anisotropic lattices) (*124*). Laser-printed anisotropy can be alleviated by a robust optimization algorithm development for design, by a material and microstructure homogenization, and by a laser printing strategy and parameter control (*124*). The third gap is reflected by the current practice in which the designs for laser-metal AM are usually oriented toward mechanical properties or limited functions, and the functionalization of AM components needs to be further enriched to strengthen the diversity of functions (Fig. 4G).

Realizing MSPI-AM

The complexity of parameters is intrinsic to AM, and an entire AM chain includes nearly 130 input- and influencing parameters (*5*). A MSPI-AM implies a comprehensive integration of various elements and parameters of material, structure, and performance/function within a monolithic component, and its implementation approaches generally include two levels: the internal coordination of individual elements and their mutual integration.

Nano- and microscale material control

The fundamental unit of a printed component is the grains and their microstructures of the material, with the length scale ranging from several nanometers to submillimeter scale (*58*, *59*). The atomic-scale structures [e.g., nanoprecipitates (*60*–*62*), supersaturated solid solution (*125*), solute microsegregation (*59*), and atomic-scale impurities (*58*)], as the minimum hierarchy of AM microstructures, normally play an underlying role in determining the performance of laser-printed metallic materials. The material-related approaches for MSPI-AM are typically realized within a nano- or microscale by controlling phases, microstructures, and interfaces. First, the homogenization of each individual material (i.e., grain structure homogeneity) through material design and process optimization is the basis for multimaterial printing and integration within a single component (Fig. 5A). Generally, laser-tailored formation of fully equiaxed, homogeneous fine grains is favorable for high-performance laser-metal AM (*63*, *126*). Assembling nanoparticles onto aluminum-based (*63*, *79*), nickel-based (*78*), or iron-based (*127*) powder to prepare nanocomposites demonstrates its feasibility, which is attributed to the mechanisms of increased nucleation sites and grain-growth retardation. Alloying is an alternative method to improve crystallization behavior for metals without grain refiner. An example is laser-printed titanium-copper alloys having a high constitutional supercooling capacity, which offsets the negative effect of a laser-induced high thermal gradient and ensures a complete columnar-to-equiaxed transition (*126*). The incorporation of external energy fields [e.g., high-intensity ultrasound (*128*) and strong magnetic field (*129*)] during AM also yields fully equiaxed grains and improved mechanical properties without changing material composition.

Second, tailoring a sound compatibility between multiple materials further strengthens multimaterial integration through interfacial coherence and its control (Fig. 5B). A simultaneous occurrence of the melting/solidification transformation of the current printing material and the cyclic reheating and solid-state phase transformation in the previously printed materials (so-called "intrinsic heat treatment") generates hierarchical phases and microstructures (*59*) and complex residual stresses (*9*, *130*). MSPI-AM calls for a metallurgically coherent intermaterial interface free of defects such as voids, cracks, and incomplete fusion (*91*, *92*, *95*), as well as an atomic-scale coherent interphase interface with minimal lattice misfit (*80*) for performance/function enhancement. Therefore, a multimaterial combination with sufficiently high mutual wettability is preferred (*131*, *132*) and the individualized printing parameters can be optimized to correspond to specific materials (*89*, *91*, *93*, *96*), thereby improving interphase/intermaterial interfacial coherence in the printed components. LDED of copper-nickel with improved wettability yields nearly full densification and a defect-free Cu-Ni graded structure (*131*), whereas the homogeneous melting tracks cannot be produced during LPBF of Ag/SnO_2 contact material as a result of insufficient wettability (*132*).

Third, because the multimaterials are normally presented in different structural forms, an ultimate important material-related approach for MSPI-AM is to build the correlation between materials and structures to adapt to a specific performance or function. The main considerations are (i) the applicability of the chemical compositions, physical properties, and mechanical properties of a specific material system to the designed structure and performance, and (ii) the attendant (sufficiently high) material/structure printability. A typical example is the LDED process for porous Ti-Ta alloys coating on a Ti6Al4V acetabular cup (Fig. 5C), which incorporates the excellent biocompatibility of Ta and the good mechanical properties and processability of Ti. LDED-printed Ti-Ta alloys incorporate microporosities during processing, as well as in situ nanoscale surface modification to enhance both in vitro cytocompatibility and early-stage in vivo osseointegration (*133*). Another example highlighting the contribution of material selection to the printed function is the bimetallic LPBF approach to embedding dissimilar tagging material (Cu10Sn copper alloy) safety features into 316L stainless steel components. The heavier atomic weight of the tagging material and its thicker printed layer contribute to higher contrast in digital x-ray images, enabling effective identification of the embedded tags (*134*).

Mesoscale process control

A successful realization of MSPI-AM relies directly on a tailored laser AM process. The length scales of process-related physical metallurgical phenomena are typically at the "mesoscale," between the material-related microscale and the component-related macroscale. MSPI-AM requires precise control of an entirely interconnected process chain, involving four sequentially dependent scientific issues (Fig. 5, D to G), which relies on high-fidelity mesoscale simulations and technical control of heat transfer, thermodynamics, and fluid dynamics during AM. First, the interaction of the laser with the matter being printed directly determines whether printing can be initiated. For LPBF, as a consequence of multiple reflections in open pores throughout the powder layer, laser energy penetrates to a depth much greater than the powder scale until finally reaching the underlying printed layer (*135*–*137*). For LDED, the laser beam generates a melt pool on a substrate where the filler material (typically powder) is injected. The laser goes through a cloud of injected powder, during which a substantial percentage of energy is absorbed by the powder. Absorptivity varies in a complicated way as a function of particle morphology before melting (*138*), melt pool morphology after melting, and real-time processing temperature (*136*, *139*). The effective absorptivity of powder under a wide range of laser powers is affected by the transition from conduction-mode melting at low power to the keyhole mode at high power (*139*, *140*). The absorptivity increases with laser power, because a widening depression of melt at a higher power can accommodate more reflections with more energy absorption events (*139*). At the higher powers beyond the keyhole transition, a saturation value in absorptivity is reached. A sharp decrease in absorptivity occurs when full melting of the powder tracks occurs, followed by a keyhole-driven increase at even higher powers (*136*).

Second, energy absorption follows more complex physical processes of powder melting, melt pool formation, and defects such as spatter (*139*), denudation (*141*), and keyhole-induced porosities (*142*). In terms of modeling methodologies, high-fidelity numerical simulations

Downloaded from https://www.science.org on June 14, 2022

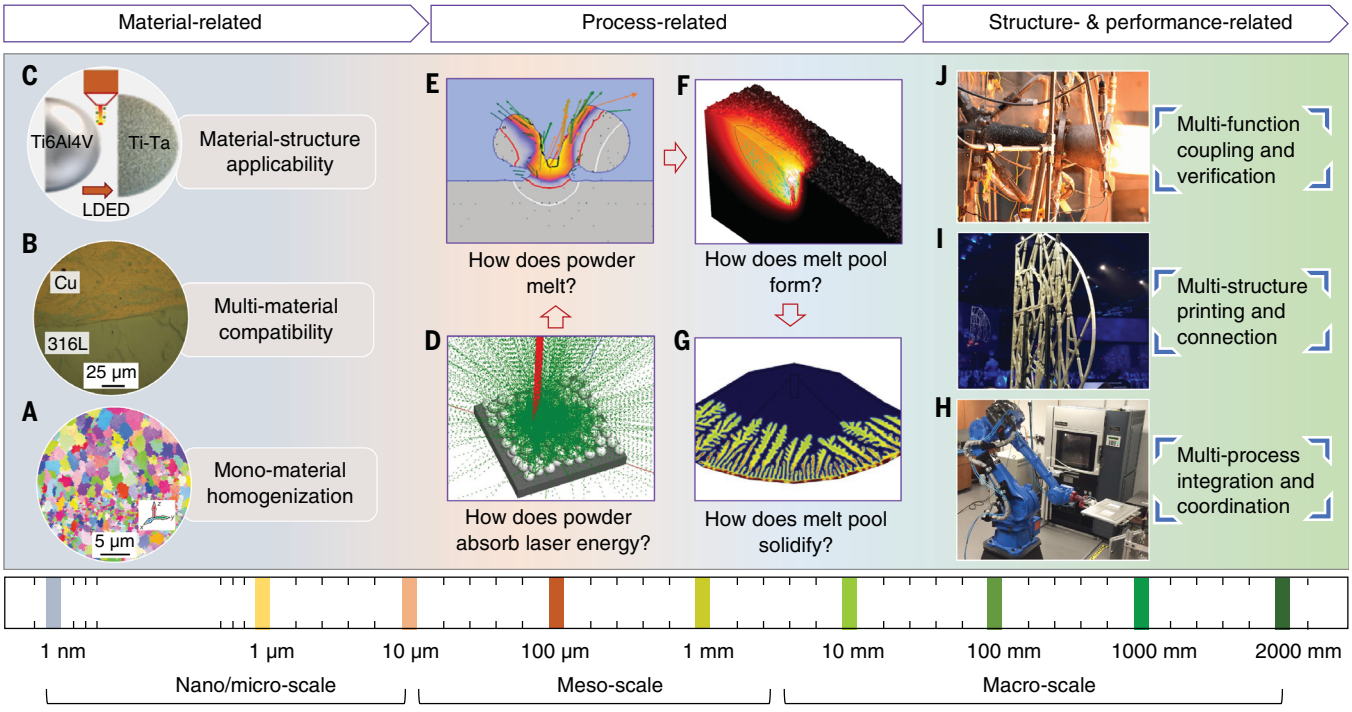

Fig. 5. Cross-scale coordination and implementation approaches for MSPI-AM of metallic components. (**A** to **C**) Material-related approaches, typically implemented on a nano- or microscale, including (A) microstructural homogenization of a specific printed material (e.g., tailoring fine equiaxed grains in LPBF zirconium nanoparticle–functionalized Al7075 aluminum alloy), (B) interfacial compatibility between multiple printed materials (e.g., forming a metallurgically adherent interface in LPBF 316L/Cu bimetallic structure), and (C) applicability of printed materials to specific structures and functions (e.g., LDED-processed porous Ti-Ta alloy coating on a Ti6Al4V acetabular cup to improve biocompatibility [images (A) to (C) reproduced from (*63*), (*95*), and (*133*), respectively, with permission]. (**D** to **G**) Process enhancement via mesoscale control of an entire laser AM of metal powder, in terms of (D) laser absorption behavior of particles, (E) powder melting behavior, (F) formation mechanism of melt pool, and (G) solidification behavior of melt pool [images (D) to (G) reproduced from (*137*), (*141*), (*142*), and (*152*), respectively, with permission]. (**H** to **J**) Macroscale structure and performance control approaches, including (H) multiprocess printing with collaborative 3D printers and a six-axis robot for conveyance and postprocess assembly, (I) laser-printed large-sized airplane cabin component with multistructures mimicking the organic cellular structure and bone growth found in living organisms, and (J) hot-fire testing of mechanical and thermal multifunctions of additive manufactured Cu/Inconel 625 bimetallic combustion chamber and nozzle for liquid rocket engines [images (H) to (J) adapted from (*34*), (*161*), and (*166*), respectively, with permission].

such as finite-element simulation for thermal modeling (*143*), computational fluid dynamics calculation for melt dynamics (*144*), and multiphase flow modeling for spattering and denudation (*145*) help to improve the fundamental understanding of the physical mechanisms for these phenomena. Recoil pressure and Marangoni convection are important in shaping the melt pool flow and determining how denudation, spatter, and pore defects emerge during LPBF (*139*–*145*). Spattering is a combined effect of the jetting vapor and attendant vortex flow of ambient gas, whereas denudation is driven by the vortex flow of ambient gas, where particles close to the vapor jet are entrained inward (*145*). The laser-spatter interaction affects the printed track quality by increasing the melt pool depth fluctuations (*139*). A low laser power fails to expel the cluster of spatters. Instead, the laser boils the top surface of the cluster and the recoil pressure presses it down into the melt pool. This outcome is problematic because it decreases the melt depth, distorts the track direction, and causes discontinuity and lack-of-fusion defects. Therefore, a sufficiently high laser power is necessary to activate the expulsion mechanism that pushes away large spatters and suppresses the associated defects (*139*).

The direct experimental approach by in situ high-speed synchrotron x-ray imaging (*139*, *140*, *146*–*149*) provides the advanced technical means to capture the rapid changes in these highly dynamic phenomena with high spatial and temporal resolution (*147*, *148*), revealing different paradigms and mechanisms for process control of these defects (*148*). Direct visualization reveals that the keyholes are present across the entire range of currently typical values of laser power and scan speed applied in LPBF. A well-defined threshold of laser power density (~0.4 MW/cm^2) exists from conduction mode to the keyhole regime, following the sequence of vaporization, depression of liquid surface, instability, and deep keyhole (*140*). The deep and narrow keyholes are responsible for the formation of some small and often spherical pores, caused by a newly discovered mechanism termed "critical instability at moving keyhole tip" (*149*). This keyhole instability generates acoustic waves in the melt pool that provide driving force for the pores near the keyhole tip to move away from the keyhole and become trapped as pores (*149*). Although the keyholes exist under essentially all typical processing conditions relevant to LPBF (*140*), the high laser energy intensity is typically required for certain AM practices; high densification of parts (>99%) can be obtained by decreasing keyhole-induced pore defects (*139*).

Third, laser-induced solidification behavior of the melt pool eventually determines a metallurgically sound printed component. Multibranched crystal formations of columnar grains or dendrites and resultant potential porosities and cracks are not acceptable for engineering applications (*150*). Laser-controlled solidification is completed by three major events of heterogeneous nucleation of melt, grain growth and microstructure development, and mushy-zone heat/mass transfer and densification (*151*, *152*).

Downloaded from https://www.science.org on June 14, 2022

Normally, an increase of laser energy lowers residual porosity but intensifies grain growth (*153*). Critical energy densities need to be tailored to balance the competition between densification activity and grain coarsening, simultaneously achieving full density, grain refinement, and elevated printability (*154*, *155*).

Macroscale structure and performance control

The ultimate realization of MSPI-AM is embodied by the printed components and their structures to meet industrial application requirements, which are normally several millimeters to a few meters in size. First, MSPI-AM of an integral component with a great deal of structural complexity calls for multiprocess printing with collaborative use of various processes (Fig. 5H) (*34*). The combination of multiple AM processes with other complementary manufacturing processes [e.g., machining (*156*), assembly (*157*), cold spraying (*158*), laser shock peening (*159*), electropulsing (*160*), etc.] is necessary to realize the spatial control of multimaterial layout, multistructure geometries, and multifunctionality.

Second, MSPI-AM requires the integration of multiple structures, which is implemented by both the overall structural design and the precise structural control during printing. A laser-printed large-scale airplane cabin component to separate the passenger cabin from the galley (i.e., a "bionic partition") (Fig. 5I) presents a typical example of multistructure integration in aircraft manufacturing to solve the major engineering puzzle of minimizing weight while retaining maximal infrastructure safety. This innovative bioinspired design capitalizes on the power of cloud computing to generate thousands of design alternatives to meet specific goals and constraints (*161*). Multistructure integration is strongly dependent on the structural accuracy, which is controlled by the residual stresses and resultant deformation of printed structures. Essentially, residual stresses during laser AM can be reduced by weakening local thermal gradients in the melt pool, which can be accomplished by (i) preheating the substrate and previously deposited layers (*9*, *17*, *162*), (ii) optimizing laser printing parameters to maintain constant melt pool morphology/size, especially at the corners of printing areas (*163*); and (iii) setting up a proper laser scanning pattern by dividing cross sections into islands to reduce vector length (so-called "island scanning" strategy) (*164*) and shifting the position of scan vectors in each island between neighboring layers (*80*, *164*, *165*).

Third, the final realization of MSPI-AM relies on multifunction coupling in an integral component and systematic function verification in a real/close-to-real service environment. Aerospace components generally require aggressive testing conditions to demonstrate multifunctionality and survivability in the harsh service environment. For example, hot-fire testing was completed on LDED-fabricated multialloy integrated-channel nozzles, accumulating a total of 142 tests over a period of 5242 s (Fig. 5J); this testing advanced the design and AM technologies for regeneratively cooled thrust chamber assemblies of liquid rocket engines (*166*). The continuous monitoring, measurement, feedback, and control of both AM process and printed components guarantee the application maturity of AM technologies. The current AM process monitoring mainly focuses on the in situ powder flow rate and distribution (*167*, *168*), melt pool temperature and melt surface characteristics (*169*, *170*), and layerwise anomaly and porosity defects (*171*, *172*). Process monitoring solutions need to be combined with nondestructive testing data taken from printed components (e.g., dimensional accuracy, surface finish, internal structure and defects, chemical compositions, and residual stresses) (*173*) and their service performance data under real situations, so as to generate intervention and acceptance limits for defect types, morphologies, and dimensions and to increase the number of methods for their elimination (*5*).

The outlook for enhancing MSPI-AM

MSPI-AM is still evolving from a concept to a practical methodology that contributes to the high-performance/multifunctional goals of AM. Because of the rich scientific and technological connotations and multidisciplinary characteristics of AM technologies, many opportunities exist for further enhancements of MSPI-AM to provide other advances in scientific discovery, technological breakthroughs, and industrial applications of AM technologies. We highlight some trends and development frontiers.

An enhanced MSPI-AM relies on a more digitized material development and printing. The vast majority of the more than 5500 alloys in use today cannot be reliably printed because of metallurgical defects (*63*) and, consequently, the next-generation metallic materials for AM become even more difficult to process. The even bigger challenge is that the different categories of difficult-to-process materials are expected to be printed within an integral component to achieve 3D-gradient distribution with high-performance/multifunctional outcomes. The design and preparation of AM-applicable materials can be accelerated through data-driven, complementary efforts in theory, computation, and experiments, thereby revealing the underlying structure-performance relationships intrinsic to a materials genome. The combination of the Materials Genome Initiative (MGI) (*174*) with AM accordingly advances a paradigm for materials discovery and design. Digitizing materials information with standardized formats for data and metadata to accelerate data aggregation should facilitate the development of tools to automate the synthesis and characterization of AM materials. The emergence of metamaterials also promotes the digitization of materials (*54*, *175*, *176*), contributing to the development of "materials" that are not yet available. Metamaterials with precisely designed artificial structures demonstrate extraordinary physical properties that natural materials do not have, substantially enriching the connotation of "material." The functionalization of metamaterials depends on a high structure resolution of the printed components (*54*, *175*, *176*), which further requires development of printing matter, improved laser resources, and different printing equipment and methods. Structures for laser-metal AM are developing toward two extremes of larger or smaller to meet the multifunctional requirements of an enhanced MSPI-AM. The dimension of large-scale metallic components produced by LDED exceeds 3 m (*177*), whereas the structural resolution of micro-LPBF for metals is as low as 30 μm (*178*). These size limits will continue to be exceeded. As an ultimate form of digitized printing, the establishment of a systematic printability database helps to enhance MSPI-AM with autonomous decision-making from the printing systems, bringing together the appropriate functional modules of materials, structures, and process approaches as well as potential defect categories, performance levels, and control measures.

MSPI-oriented AM becomes more intelligent in processes and production. The digitally designed and optimized new materials and structures for AM further bring challenges to process approaches and their control methods. Laser AM processes are becoming much more intelligent to meet the demands for customized, high-quality products in highly variable batches with short delivery times. One of the latest and most exciting frontiers in intelligent AM is the concept of digital twins (*9*, *179*). By incorporating multiphysics simulations, intelligent sensing on real-time objects, big-data statistics and analytics, and machine learning capabilities, digital twins demonstrate great potential in (i) the efficient design of new products for AM, (ii) AM production planning (with respect to usage scenarios and environmental conditions), and (iii) the capture, analysis, and action on AM operational data and final high quality. The collected big data play a fundamental role in improving the intelligence of MSPI-AM technologies. At the level of the individual printer, to ensure accurate prediction and control over an entire process of AM production, big data from sensors installed on the printer and objects being printed are fundamentally important to determine the real-time process situations and their changes over time. For the level of multiprinter and data integration and by integrating more data collected from a vast number of printers, a

Downloaded from https://www.science.org on June 14, 2022

big data–driven framework can be further developed to enable a more intelligent AM with improved productivity and quality (*180*). The new-generation laser-metal printers accordingly need to integrate more intelligent detection, sensing, and monitoring devices, such as in situ, high-speed, high-resolution imaging systems to capture the dynamics of laser AM (*167*, *169*, *170*) and nondestructive detection systems to quantify porosity, residual stresses, deformation, and other defects (*173*).

The diversification of approaches is necessary for further enhancing MSPI-AM. One of the most important outcomes of MSPI-AM is the wide integration of multifunctions within an integral component, yielding both mechanical performance and sound, light, magnetic, electrical, and thermal-related functions. The approaches to achieve the final goals of MSPI-AM accordingly become more hybrid (*34*). First, materials selection and solutions become more versatile to realize MSPI-AM. For example, the local replacement of a fraction of metallic components with a material having a higher strength-to-weight ratio, such as carbon fiber composites, provides a substantial weight savings opportunity in aerospace manufacturing fields, which further calls for non–metal-based 3DP technologies and their coordination with metal-based printing. The second consideration in MSPI-AM is to strengthen the integration of various AM technologies and complementary processes to navigate complex printing of objects with more extreme conditions in materials and structures. Third, because of the elevated complexity of multiprocesses, a smooth interconnection of various process interfaces is favored for MSPI-AM to avoid the potential formation of defects. "Virtual manufacturing" based on numerical simulations can be integrated with real production to promote MSPI-AM, providing the multiscale modeling and accurate prediction of an entire AM process and attendant optimization of printing techniques and parameters. The advanced computational algorithms and codes, high-performance computing methods, and innovations in process control methods are required to achieve a component-scale understanding of basic physics and technical methodologies of laser AM production with a substantial process enhancement.

REFERENCES AND NOTES

1. K. Lu, The future of metals. *Science* **328**, 319–320 (2010). doi: 10.1126/science.1185866; pmid: 20395503
2. D. Raabe, C. C. Tasan, E. A. Olivetti, Strategies for improving the sustainability of structural metals. *Nature* **575**, 64–74 (2019). doi: 10.1038/s41586-019-1702-5; pmid: 31695209
3. T. M. Pollock, Weight loss with magnesium alloys. *Science* **328**, 986–987 (2010). doi: 10.1126/science.1182848; pmid: 20489013
4. D. L. Bourell, D. W. Rosen, M. C. Leu, The roadmap for additive manufacturing and its impact. *3D Print. Addit. Manuf.* **1**, 6–9 (2014). doi: 10.1089/3dp.2013.0002
5. M. Schmidt *et al*., Laser based additive manufacturing in industry and academia. *CIRP Ann. Manuf. Technol.* **66**, 561–583 (2017). doi: 10.1016/j.cirp.2017.05.011
6. T. DebRoy *et al*., Scientific, technological and economic issues in metal printing and their solutions. *Nat. Mater.* **18**, 1026–1032 (2019). doi: 10.1038/s41563-019-0408-2; pmid: 31263223
7. F. Froes, R. Boyer, *Additive Manufacturing for the Aerospace Industry* (Elsevier, 2019).
8. ISO/ASTM International, *ISO/ASTM 52900. Additive Manufacturing—General Principles—Terminology* (2015).
9. T. DebRoy, T. Mukherjee, H. L. Wei, J. W. Elmer, J. O. Milewski, Metallurgy, mechanistic models and machine learning in metal printing. *Nat. Rev. Mater.* **6**, 48–68 (2021). doi: 10.1038/s41578-020-00236-1
10. S. Y. Liu, Y. C. Shin, Additive manufacturing of Ti6Al4V alloy: A review. *Mater. Des.* **164**, 107552 (2019). doi: 10.1016/j.matdes.2018.107552
11. C. T. Kwok, H. C. Man, F. T. Cheng, K. H. Lo, Developments in laser-based surface engineering processes: With particular reference to protection against cavitation erosion. *Surf. Coat. Technol.* **291**, 189–204 (2016). doi: 10.1016/j.surfcoat.2016.02.019
12. M. Perini, P. Bosetti, N. Balc, Additive manufacturing for repairing: From damage identification and modeling to DLD. *Rapid Prototyp. J.* **26**, 929–940 (2020). doi: 10.1108/RPJ-03-2019-0090
13. M. Matsumoto, S. S. Yang, K. Martinsen, Y. Kainuma, Trends and research challenges in remanufacturing. *Int. J. Precis. Eng. Manuf. Green Technol.* **3**, 129–142 (2016). doi: 10.1007/s40684-016-0016-4
14. S. E. Brika, M. Letenneur, C. A. Dion, V. Brailovski, Influence of particle morphology and size distribution on the powder flowability and laser powder bed fusion manufacturability of Ti-6Al-4V alloy. *Addit. Manuf.* **31**, 100929 (2020). doi: 10.1016/j.addma.2019.100929
15. GE Additive Machines, X Line 2000R; www.ge.com/additive/additive-manufacturing/machines/dmlm-machines/x-line-2000r.
16. M. Zastrow, 3D printing gets bigger, faster and stronger. *Nature* **578**, 20–23 (2020). doi: 10.1038/d41586-020-00271-6; pmid: 32025009
17. T. DebRoy *et al*., Additive manufacturing of metallic components – Process, structure and properties. *Prog. Mater. Sci.* **92**, 112–224 (2018). doi: 10.1016/j.pmatsci.2017.10.001
18. D. Bourell *et al*., Materials for additive manufacturing. *CIRP Ann. Manuf. Technol.* **66**, 659–681 (2017). doi: 10.1016/j.cirp.2017.05.009
19. P. C. Collins, D. A. Brice, P. Samimi, I. Ghamarian, H. L. Fraser, Microstructural control of additively manufactured metallic materials. *Annu. Rev. Mater. Res.* **46**, 63–91 (2016). doi: 10.1146/annurev-matsci-070115-031816
20. E. O. Olakanmi, R. F. Cochrane, K. W. Dalgarno, A review on selective laser sintering/melting (SLS/SLM) of aluminium alloy powders: Processing, microstructure, and properties. *Prog. Mater. Sci.* **74**, 401–477 (2015). doi: 10.1016/j.pmatsci.2015.03.002
21. W. E. King *et al*., Laser powder bed fusion additive manufacturing of metals; physics, computational, and materials challenges. *Appl. Phys. Rev.* **2**, 041304 (2015). doi: 10.1063/1.4937809
22. M. Markl, C. Körner, Multiscale modeling of powder bed–based additive manufacturing. *Annu. Rev. Mater. Res.* **46**, 93–123 (2016). doi: 10.1146/annurev-matsci-070115-032158
23. J. Smith *et al*., Linking process, structure, property, and performance for metal-based additive manufacturing: Computational approaches with experimental support. *Comput. Mech.* **57**, 583–610 (2016). doi: 10.1007/s00466-015-1240-4
24. S. Shao, M. M. Khonsari, S. Guo, W. J. Meng, N. Li, Overview: Additive manufacturing enabled accelerated design of Ni-based alloys for improved fatigue life. *Addit. Manuf.* **29**, 100779 (2019). doi: 10.1016/j.addma.2019.100779
25. A. Bandyopadhyay, B. Heer, Additive manufacturing of multi-material structures. *Mater. Sci. Eng. Rep.* **129**, 1–16 (2018). doi: 10.1016/j.mser.2018.04.001
26. N. T. Aboulkhair *et al*., 3D printing of Aluminium alloys: Additive Manufacturing of Aluminium alloys using selective laser melting. *Prog. Mater. Sci.* **106**, 100578 (2019). doi: 10.1016/j.pmatsci.2019.100578
27. M. Elahinia *et al*., Fabrication of NiTi through additive manufacturing: A review. *Prog. Mater. Sci.* **83**, 630–663 (2016). doi: 10.1016/j.pmatsci.2016.08.001
28. S. Gorsse, C. Hutchinson, M. Gouné, R. Banerjee, Additive manufacturing of metals: A brief review of the characteristic microstructures and properties of steels, Ti-6Al-4V and high-entropy alloys. *Sci. Technol. Adv. Mater.* **18**, 584–610 (2017). doi: 10.1080/14686996.2017.1361305; pmid: 28970868
29. M. K. Thompson *et al*., Design for Additive Manufacturing: Trends, opportunities, considerations, and constraints. *CIRP Ann. Manuf. Technol.* **65**, 737–760 (2016). doi: 10.1016/j.cirp.2016.05.004
30. T. Vaneker, A. Bernard, G. Moroni, I. Gibson, Y. Zhang, Design for additive manufacturing: Framework and methodology. *CIRP Ann. Manuf. Technol.* **69**, 578–599 (2020). doi: 10.1016/j.cirp.2020.05.006
31. L. Meng *et al*., From topology optimization design to additive manufacturing: Today's success and tomorrow's roadmap. *Arch. Comput. Methods Eng.* **27**, 805–830 (2020). doi: 10.1007/s11831-019-09331-1
32. J. Plocher, A. Panesar, Review on design and structural optimisation in additive manufacturing: Towards next-generation lightweight structures. *Mater. Des.* **183**, 108164 (2019). doi: 10.1016/j.matdes.2019.108164
33. H. L. Wei *et al*., Mechanistic models for additive manufacturing of metallic components. *Prog. Mater. Sci.* **116**, 100703 (2021). doi: 10.1016/j.pmatsci.2020.100703
34. E. MacDonald, R. Wicker, Multiprocess 3D printing for increasing component functionality. *Science* **353**, aaf2093 (2016). doi: 10.1126/science.aaf2093; pmid: 27708075
35. E. Hosseini, V. A. Popovich, A review of mechanical properties of additively manufactured Inconel 718. *Addit. Manuf.* **30**, 100877 (2019). doi: 10.1016/j.addma.2019.100877
36. M. Benedetti *et al*., Architected cellular materials: A review on their mechanical properties towards fatigue-tolerant design and fabrication. *Mater. Sci. Eng. Rep.* **144**, 100606 (2021). doi: 10.1016/j.mser.2021.100606
37. S. A. M. Tofail *et al*., Additive manufacturing: Scientific and technological challenges, market uptake and opportunities. *Mater. Today* **21**, 22–37 (2018). doi: 10.1016/j.mattod.2017.07.001
38. N. Tepylo, X. Huang, P. C. Patnaik, Laser-based additive manufacturing technologies for aerospace applications. *Adv. Eng. Mater.* **21**, 1900617 (2019). doi: 10.1002/adem.201900617
39. C. X. Li, D. Pisignano, Y. Zhao, J. J. Xue, Advances in medical applications of additive manufacturing. *Engineering* **6**, 1222–1231 (2020). doi: 10.1016/j.eng.2020.02.018
40. B. H. Lu, D. C. Li, X. Y. Tian, Development trends in additive manufacturing and 3D printing. *Engineering* **1**, 85–89 (2015). doi: 10.15302/J-ENG-2015012
41. O. O. Salman *et al*., Selective laser melting of 316L stainless steel: Influence of TiB_2 addition on microstructure and mechanical properties. *Mater. Today Commun.* **21**, 100615 (2019). doi: 10.1016/j.mtcomm.2019.100615
42. G. Y. Ma *et al*., High-mass-proportion TiCp/Ti6Al4V titanium matrix composites prepared by directed energy deposition. *Addit. Manuf.* **35**, 101323 (2020). doi: 10.1016/j.addma.2020.101323
43. T. Zhao *et al*., Laser metal deposition for additive manufacturing of AA5024 and nanoparticulate TiC modified AA5024 alloy composites prepared with balling milling process. *Opt. Laser Technol.* **131**, 106438 (2020). doi: 10.1016/j.optlastec.2020.106438
44. X. P. Li *et al*., Selective laser melting of nano-TiB_2 decorated AlSi10Mg alloy with high fracture strength and ductility. *Acta Mater.* **129**, 183–193 (2017). doi: 10.1016/j.actamat.2017.02.062
45. K. D. Traxel, A. Bandyopadhyay, Influence of in situ ceramic reinforcement towards tailoring titanium matrix composites using laser-based additive manufacturing. *Addit. Manuf.* **31**, 101004 (2020). doi: 10.1016/j.addma.2019.101004; pmid: 32864348
46. Q. Q. Han *et al*., Selective laser melting of Hastelloy X nanocomposite: Effects of TiC reinforcement on crack elimination and strength improvement. *Composites B* **202**, 108442 (2020). doi: 10.1016/j.compositesb.2020.108442
47. A. Reichardt *et al*., Advances in additive manufacturing of metal-based functionally graded materials. *Int. Mater. Rev.* **66**, 1–29 (2021). doi: 10.1080/09506608.2019.1709354
48. L. Yan, Y. T. Chen, F. Liou, Additive manufacturing of functionally graded metallic materials using laser metal deposition. *Addit. Manuf.* **31**, 100901 (2020). doi: 10.1016/j.addma.2019.100901

Downloaded from https://www.science.org on June 14, 2022

49. L. Berrocal *et al*., Topology optimization and additive manufacturing for aerospace components. *Prog. Addit. Manuf.* **4**, 83–95 (2019). doi: 10.1007/s40964-018-0061-3
50. J. H. Zhu *et al*., A review of topology optimization for additive manufacturing: Status and challenges. *Chin. J. Aeronaut.* **34**, 91–110 (2021). doi: 10.1016/j.cja.2020.09.020
51. M. Eder, S. Amini, P. Fratzl, Biological composites—complex structures for functional diversity. *Science* **362**, 543–547 (2018). doi: 10.1126/science.aat8297; pmid: 30385570
52. Y. Yang *et al*., Recent progress in biomimetic additive manufacturing technology: From materials to functional structures. *Adv. Mater.* **30**, e1706539 (2018). doi: 10.1002/adma.201706539; pmid: 29920790
53. A. Nazir, K. M. Abate, A. Kumar, J. Y. Jeng, A state-of-the-art review on types, design, optimization, and additive manufacturing of cellular structures. *Int. J. Adv. Manuf. Technol.* **104**, 3489–3510 (2019). doi: 10.1007/s00170-019-04085-3
54. X. Zheng *et al*., Multiscale metallic metamaterials. *Nat. Mater.* **15**, 1100–1106 (2016). doi: 10.1038/nmat4694; pmid: 27429209
55. H. Ghasemi-Tabasi *et al*., An effective rule for translating optimal selective laser melting processing parameters from one material to another. *Addit. Manuf.* **36**, 101496 (2020). doi: 10.1016/j.addma.2020.101496
56. H. C. Tran, Y. L. Lo, Systematic approach for determining optimal processing parameters to produce parts with high density in selective laser melting process. *Int. J. Adv. Manuf. Technol.* **105**, 4443–4460 (2019). doi: 10.1007/s00170-019-04517-0
57. M. Juhasz *et al*., Hybrid directed energy deposition for fabricating metal structures with embedded sensors. *Addit. Manuf.* **35**, 101397 (2020). doi: 10.1016/j.addma.2020.101397
58. Y. M. Wang *et al*., Additively manufactured hierarchical stainless steels with high strength and ductility. *Nat. Mater.* **17**, 63–71 (2018). doi: 10.1038/nmat5021; pmid: 29115290
59. P. Kürnsteiner *et al*., High-strength Damascus steel by additive manufacturing. *Nature* **582**, 515–519 (2020). doi: 10.1038/s41586-020-2409-3; pmid: 32581379
60. A. B. Spierings, K. Dawson, P. Dumitraschkewitz, S. Pogatscher, K. Wegener, Microstructure characterization of SLM-processed Al-Mg-Sc-Zr alloy in the heat treated and HIPed condition. *Addit. Manuf.* **20**, 173–181 (2018). doi: 10.1016/j.addma.2017.12.011
61. R. D. Li *et al*., Developing a high-strength Al-Mg-Si-Sc-Zr alloy for selective laser melting: Crack-inhibiting and multiple strengthening mechanisms. *Acta Mater.* **193**, 83–98 (2020). doi: 10.1016/j.actamat.2020.03.060
62. Q. Jia *et al*., Precipitation kinetics, microstructure evolution and mechanical behavior of a developed Al-Mn-Sc alloy fabricated by selective laser melting. *Acta Mater.* **193**, 239–251 (2020). doi: 10.1016/j.actamat.2020.04.015; pmid: 33093793
63. J. H. Martin *et al*., 3D printing of high-strength aluminium alloys. *Nature* **549**, 365–369 (2017). doi: 10.1038/nature23894; pmid: 28933439
64. P. Barriobero-Vila *et al*., Peritectic titanium alloys for 3D printing. *Nat. Commun.* **9**, 3426 (2018). doi: 10.1038/s41467-018-05819-9; pmid: 30143641
65. C. Han *et al*., Recent advances on high-entropy alloys for 3D printing. *Adv. Mater.* **32**, e1903855 (2020). doi: 10.1002/adma.201903855; pmid: 32431005
66. C. Zhang *et al*., A review on microstructures and properties of high entropy alloys manufactured by selective laser melting. *Int. J. Extrem. Manuf.* **2**, 032003 (2020). doi: 10.1088/2631-7990/ab9ead
67. P. Agrawal *et al*., Excellent strength-ductility synergy in metastable high entropy alloy by laser powder bed additive manufacturing. *Addit. Manuf.* **32**, 101098 (2020). doi: 10.1016/j.addma.2020.101098
68. M. S. K. K. Y. Nartu *et al*., Magnetic and mechanical properties of an additively manufactured equiatomic CoFeNi complex concentrated alloy. *Scr. Mater.* **187**, 30–36 (2020). doi: 10.1016/j.scriptamat.2020.05.063
69. M. A. Melia *et al*., Mechanical and corrosion properties of additively manufactured CoCrFeMnNi high entropy alloy. *Addit. Manuf.* **29**, 100833 (2019). doi: 10.1016/j.addma.2019.100833
70. M. Jin *et al*., Cyclic plasticity and fatigue damage of CrMnFeCoNi high entropy alloy fabricated by laser powder-bed fusion. *Addit. Manuf.* **36**, 101584 (2020). doi: 10.1016/j.addma.2020.101584
71. Y.-K. Kim, S. S. Yang, K.-A. Lee, Compressive creep behavior of selective laser melted CoCrFeMnNi high-entropy alloy strengthened by in-situ formation of nano-oxides. *Addit. Manuf.* **36**, 101543 (2020). doi: 10.1016/j.addma.2020.101543
72. S. Thapliyal *et al*., Damage-tolerant, corrosion-resistant high entropy alloy with high strength and ductility by laser powder bed fusion additive manufacturing. *Addit. Manuf.* **36**, 101455 (2020). doi: 10.1016/j.addma.2020.101455
73. A. Mohanty *et al*., High temperature oxidation study of direct laser deposited AlXCoCrFeNi (X=0.3,0.7) high entropy alloys. *Surf. Coat. Technol.* **380**, 125028 (2019). doi: 10.1016/j.surfcoat.2019.125028
74. H. Wang *et al*., Effect of cyclic rapid thermal loadings on the microstructural evolution of a CrMnFeCoNi high-entropy alloy manufactured by selective laser melting. *Acta Mater.* **196**, 609–625 (2020). doi: 10.1016/j.actamat.2020.07.006
75. T. C. Lin *et al*., Aluminum with dispersed nanoparticles by laser additive manufacturing. *Nat. Commun.* **10**, 4124 (2019). doi: 10.1038/s41467-019-12047-2; pmid: 31511518
76. L. F. Liu *et al*., Dislocation network in additive manufactured steel breaks strength–ductility trade-off. *Mater. Today* **21**, 354–361 (2018). doi: 10.1016/j.mattod.2017.11.004
77. D. D. Gu, J. Ma, H. Chen, K. Lin, L. Xi, Laser additive manufactured WC reinforced Fe-based composites with gradient reinforcement/matrix interface and enhanced performance. *Compos. Struct.* **192**, 387–396 (2018). doi: 10.1016/j.compstruct.2018.03.008
78. I. T. Ho, Y.-T. Chen, A.-C. Yeh, C.-P. Chen, K.-K. Jen, Microstructure evolution induced by inoculants during the selective laser melting of IN718. *Addit. Manuf.* **21**, 465–471 (2018). doi: 10.1016/j.addma.2018.02.018
79. C. Gao *et al*., Selective laser melting of TiN nanoparticle-reinforced AlSi10Mg composite: Microstructural, interfacial, and mechanical properties. *J. Mater. Process. Technol.* **281**, 116618 (2020). doi: 10.1016/j.jmatprotec.2020.116618
80. D. D. Gu *et al*., Carbon nanotubes enabled laser 3D printing of high-performance titanium with highly concentrated reinforcement. *iScience* **23**, 101498 (2020). doi: 10.1016/j.actamat.2018.03.013
81. D. Lin *et al*., Shock engineering the additive manufactured graphene-metal nanocomposite with high density nanotwins and dislocations for ultra-stable mechanical properties. *Acta Mater.* **150**, 360–372 (2018). doi: 10.1016/j.actamat.2018.03.013
82. M. Lorusso *et al*., Understanding friction and wear behavior at the nanoscale of aluminum matrix composites produced by laser powder bed fusion. *Adv. Eng. Mater.* **22**, 1900815 (2020). doi: 10.1002/adem.201900815
83. T. B. Torgerson, S. A. Mantri, R. Banerjee, T. W. Scharf, Room and elevated temperature sliding wear behavior and mechanisms of additively manufactured novel precipitation strengthened metallic composites. *Wear* **426–427**, 942–951 (2019). doi: 10.1016/j.wear.2018.12.046
84. L. Chen, Y. Z. Sun, L. Li, X. D. Ren, Effect of heat treatment on the microstructure and high temperature oxidation behavior of TiC/Inconel 625 nanocomposites fabricated by selective laser melting. *Corros. Sci.* **169**, 108606 (2020). doi: 10.1016/j.corsci.2020.108606
85. J. D. Avila, A. Bandyopadhyay, Influence of boron nitride reinforcement to improve high temperature oxidation resistance of titanium. *J. Mater. Res.* **34**, 1279–1289 (2019). doi: 10.1557/jmr.2019.11; pmid: 31406396
86. Y. J. Zhang *et al*., Corrosion mechanism of amorphous alloy strengthened stainless steel composite fabricated by selective laser melting. *Corros. Sci.* **163**, 108241 (2020). doi: 10.1016/j.corsci.2019.108241
87. J. C. Wang *et al*., Selective laser melting of Ti-35Nb composite from elemental powder mixture: Microstructure, mechanical behavior and corrosion behavior. *Mater. Sci. Eng. A* **760**, 214–224 (2019). doi: 10.1016/j.msea.2019.06.001
88. H. M. Zhang, D. Gu, C. Ma, M. Xia, M. Guo, Surface wettability and superhydrophobic characteristics of Ni-based nanocomposites fabricated by selective laser melting. *Appl. Surf. Sci.* **476**, 151–160 (2019). doi: 10.1016/j.apsusc.2019.01.060
89. Y. N. Zhang, A. Bandyopadhyay, Direct fabrication of compositionally graded Ti-Al_2O_3 multi-material structures using Laser Engineered Net Shaping. *Addit. Manuf.* **21**, 104–111 (2018). doi: 10.1016/j.addma.2018.03.001
90. X. J. Zhang, C. Wei, Y. H. Chueh, L. Li, An integrated dual ultrasonic selective powder dispensing platform for three-dimensional printing of multiple material metal/glass objects in selective laser melting. *Trans. ASME J. Manuf. Sci. Eng.* **141**, 011003 (2019). doi: 10.1115/1.4041427
91. J. Chen *et al*., Interfacial microstructure and mechanical properties of 316L/CuSn10 multi-material bimetallic structure fabricated by selective laser melting. *Mater. Sci. Eng. A* **752**, 75–85 (2019). doi: 10.1016/j.msea.2019.02.097
92. F. Brueckner *et al*., Enhanced manufacturing possibilities using multi-materials in laser metal deposition. *J. Laser Appl.* **30**, 032308 (2018). doi: 10.2351/1.5040639
93. W. Li *et al*., Fabrication and characterization of a functionally graded material from Ti-6Al-4V to SS316 by laser metal deposition. *Addit. Manuf.* **14**, 95–104 (2017). doi: 10.1016/j.addma.2016.12.006
94. D. R. Feenstra, A. Molotnikov, N. Birbilis, Effect of energy density on the interface evolution of stainless steel 316L deposited upon INC 625 via directed energy deposition. *J. Mater. Sci.* **55**, 13314–13328 (2020). doi: 10.1007/s10853-020-04913-y
95. Z. H. Liu, D. Q. Zhang, S. L. Sing, C. K. Chua, L. E. Loh, Interfacial characterization of SLM parts in multi-material processing: Metallurgical diffusion between 316L stainless steel and C18400 copper alloy. *Mater. Charact.* **94**, 116–125 (2014). doi: 10.1016/j.matchar.2014.05.001
96. C. Wei, L. Li, X. J. Zhang, Y.-H. Chueh, 3D printing of multiple metallic materials via modified selective laser melting. *CIRP Ann. Manuf. Technol.* **67**, 245–248 (2018). doi: 10.1016/j.cirp.2018.04.096
97. B. Onuike, B. Heer, A. Bandyopadhyay, Additive manufacturing of Inconel 718-Copper alloy bimetallic structure using laser engineered net shaping (LENS™). *Addit. Manuf.* **21**, 133–140 (2018). doi: 10.1016/j.addma.2018.02.007
98. R. M. Mahamood, E. T. Akinlabi, Laser metal deposition of functionally graded Ti6Al4V/TiC. *Mater. Des.* **84**, 402–410 (2015). doi: 10.1016/j.matdes.2015.06.135
99. I. Shishkovsky, N. Kakovkina, V. Sherbakov, Graded layered titanium composite structures with TiB_2 inclusions fabricated by selective laser melting. *Compos. Struct.* **169**, 90–96 (2017). doi: 10.1016/j.compstruct.2016.11.013
100. D. Lehmhus *et al*., Customized smartness: A survey on links between additive manufacturing and sensor integration. *Procedia Technol.* **26**, 284–301 (2016). doi: 10.1016/j.protcy.2016.08.038
101. D. Lehmhus, M. Busse, A. von Hehl, E. Jägle, State of the art and emerging trends in additive manufacturing: From multi-material processes to 3D printed electronics. *MATEC Web Conf.* **188**, 03013 (2018). doi: 10.1016/j.compstruct.2016.11.013
102. D. Espalin, D. W. Muse, E. MacDonald, R. B. Wicker, 3D Printing multifunctionality: Structures with electronics. *Int. J. Adv. Manuf. Technol.* **72**, 963–978 (2014). doi: 10.1007/s00170-014-5717-7
103. C. Vedder *et al*., Laser-based functionalization of electronic multi-material-layers for embedded sensors. *J. Laser Appl.* **29**, 022603 (2017). doi: 10.2351/1.4983267
104. T. Töppel *et al*., Structural integration of sensors/actuators by laser beam melting for tailored smart components. *JOM* **70**, 321–327 (2018). doi: 10.1007/s11837-017-2725-8
105. I. Dani, Smart components by additive technologies. *IOP Conf. Series Mater. Sci. Eng.* **480**, 012016 (2019). doi: 10.1088/1757-899X/480/1/012016
106. M. S. Hossain *et al*., Fabrication of smart parts using powder bed fusion additive manufacturing technology. *Addit. Manuf.* **10**, 58–66 (2016). doi: 10.1016/j.addma.2016.01.001
107. Y. K. Sui, X. R. Peng, *Modelling, Solving and Application for Topology Optimization of Continuum Structures* (Elsevier, 2018).
108. T. Gao, L. B. Qiu, W. H. Zhang, Topology optimization of continuum structures subjected to the variance constraint of reaction forces. *Struct. Multidiscipl. Optim.* **56**, 755–765 (2017). doi: 10.1007/s00158-017-1742-0
109. S. Das, A. Sutradhar, Multi-physics topology optimization of functionally graded controllable porous structures: Application to heat dissipating problems. *Mater. Des.* **193**, 108775 (2020). doi: 10.1016/j.matdes.2020.108775
110. V. Subramaniam, T. Dbouk, J. L. Harion, Topology optimization of conductive heat transfer devices: An experimental investigation. *Appl. Therm. Eng.* **131**, 390–411 (2018). doi: 10.1016/j.applthermaleng.2017.12.026
111. E. M. Dede, S. N. Joshi, F. Zhou, Topology optimization, additive layer manufacturing, and experimental testing of an air-cooled heat sink. *Trans. ASME J. Mech. Design* **137**, 111403 (2015). doi: 10.1115/1.4030989

Downloaded from https://www.science.org on June 14, 2022

112. F. García Ferré *et al*., A lightweight electromagnetic actuator for high voltage DC power grids. *Addit. Manuf.* **27**, 533–539 (2019). doi: 10.1016/j.addma.2019.03.018
113. D. M. Dattelbaum *et al*., Shockwave interactions with additively-manufactured polymer structures. *AIP Conf. Proc.* **2272**, 040002 (2020). doi: 10.1063/12.0001124
114. M. S. Pham, C. Liu, I. Todd, J. Lertthanasarn, Damage-tolerant architected materials inspired by crystal microstructure. *Nature* **565**, 305–311 (2019). doi: 10.1038/s41586-018-0850-3; pmid: 30651615
115. A. du Plessis *et al*., Beautiful and functional: A review of biomimetic design in additive manufacturing. *Addit. Manuf.* **27**, 408–427 (2019). doi: 10.1016/j.addma.2019.03.033
116. N. Aage, E. Andreassen, B. S. Lazarov, O. Sigmund, Giga-voxel computational morphogenesis for structural design. *Nature* **550**, 84–86 (2017). doi: 10.1038/nature23911; pmid: 28980645
117. M. Gralow, F. Weigand, D. Herzog, T. Wischeropp, C. Emmelmann, Biomimetic design and laser additive manufacturing—A perfect symbiosis? *J. Laser Appl.* **32**, 021201 (2020). doi: 10.2351/1.5131642
118. K. J. Lin, K. M. Hu, D. D. Gu, Metallic integrated thermal protection structures inspired by the Norway spruce stem: Design, numerical simulation and selective laser melting fabrication. *Opt. Laser Technol.* **115**, 9–19 (2019). doi: 10.1016/j.optlastec.2019.02.003
119. K. M. Hu *et al*., Mechanical properties and deformation behavior under compressive loading of selective laser melting processed bio-inspired sandwich structures. *Mater. Sci. Eng. A* **762**, 138089 (2019). doi: 10.1016/j.msea.2019.138089
120. A. Velasco-Hogan, J. Xu, M. A. Meyers, Additive manufacturing as a method to design and optimize bioinspired structures. *Adv. Mater.* **30**, e1800940 (2018). doi: 10.1002/adma.201800940; pmid: 30133816
121. T. Tancogne-Dejean, D. Mohr, Stiffness and specific energy absorption of additively-manufactured metallic BCC metamaterials composed of tapered beams. *Int. J. Mech. Sci.* **141**, 101–116 (2018). doi: 10.1016/j.ijmecsci.2018.03.027
122. C. L. Li *et al*., Crushing behavior of multi-layer metal lattice panel fabricated by selective laser melting. *Int. J. Mech. Sci.* **145**, 389–399 (2018). doi: 10.1016/j.ijmecsci.2018.07.029
123. T. Tancogne-Dejean, A. B. Spierings, D. Mohr, Additively-manufactured metallic micro-lattice materials for high specific energy absorption under static and dynamic loading. *Acta Mater.* **116**, 14–28 (2016). doi: 10.1016/j.actamat.2016.05.054
124. P. Zhang, J. K. Liu, A. C. To, Role of anisotropic properties on topology optimization of additive manufactured load bearing structures. *Scr. Mater.* **135**, 148–152 (2017). doi: 10.1016/j.scriptamat.2016.10.021
125. P. Kürnsteiner *et al*., Control of thermally stable core-shell nano-precipitates in additively manufactured Al-Sc-Zr alloys. *Addit. Manuf.* **32**, 100910 (2020). doi: 10.1016/j.addma.2019.100910
126. D. Zhang *et al*., Additive manufacturing of ultrafine-grained high-strength titanium alloys. *Nature* **576**, 91–95 (2019). doi: 10.1038/s41586-019-1783-1; pmid: 31802014
127. B. AlMangour, Y. K. Kim, D. Grzesiak, K. A. Lee, Novel TiB_2-reinforced 316L stainless steel nanocomposites with excellent room- and high-temperature yield strength developed by additive manufacturing. *Composites B* **156**, 51–63 (2019). doi: 10.1016/j.compositesb.2018.07.050
128. C. J. Todaro *et al*., Grain structure control during metal 3D printing by high-intensity ultrasound. *Nat. Commun.* **11**, 142 (2020). doi: 10.1038/s41467-019-13874-z; pmid: 31919347
129. Y. C. Wang, J. Shi, Texture control of Inconel 718 superalloy in laser additive manufacturing by an external magnetic field. *J. Mater. Sci.* **54**, 9809–9823 (2019). doi: 10.1007/s10853-019-03569-7
130. T. Mukherjee, J. S. Zuback, W. Zhang, T. DebRoy, Residual stresses and distortion in additively manufactured compositionally graded and dissimilar joints. *Comput. Mater. Sci.* **143**, 325–337 (2018). doi: 10.1016/j.commatsci.2017.11.026
131. S. Yadav, A. N. Jinoop, N. Sinha, C. P. Paul, K. S. Bindra, Parametric investigation and characterization of laser directed energy deposited copper-nickel graded layers. *Int. J. Adv. Manuf. Technol.* **108**, 3779–3791 (2020). doi: 10.1007/s00170-020-05644-9
132. S. Szemkus *et al*., Laser additive manufacturing of contact materials. *J. Mater. Process. Technol.* **252**, 612–617 (2018). doi: 10.1016/j.jmatprotec.2017.09.023
133. I. Mitra *et al*., 3D Printing in alloy design to improve biocompatibility in metallic implants. *Mater. Today* 10.1016/j.mattod.2020.11.021 (2021). doi: 10.1016/j.mattod.2020.11.021
134. C. Wei, Z. Sun, Y. H. Huang, L. Li, Embedding anti-counterfeiting features in metallic components via multiple material additive manufacturing. *Addit. Manuf.* **24**, 1–12 (2018). doi: 10.1016/j.addma.2018.09.003
135. A. V. Gusarov, J. P. Kruth, Modelling of radiation transfer in metallic powders at laser treatment. *Int. J. Heat Mass Transf.* **48**, 3423–3434 (2005). doi: 10.1016/j.ijheatmasstransfer.2005.01.044
136. J. Trapp, A. M. Rubenchik, G. Guss, M. J. Matthews, In situ absorptivity measurements of metallic powders during laser powder-bed fusion additive manufacturing. *Appl. Mater. Today* **9**, 341–349 (2017). doi: 10.1016/j.apmt.2017.08.006
137. D. D. Gu, Y. Yang, L. Xi, J. Yang, M. Xia, Laser absorption behavior of randomly packed powder-bed during selective laser melting of SiC and TiB_2 reinforced Al matrix composites. *Opt. Laser Technol.* **119**, 105600 (2019). doi: 10.1016/j.optlastec.2019.105600
138. M. A. Balbaa *et al*., Role of powder particle size on laser powder bed fusion processability of AlSi10Mg alloy. *Addit. Manuf.* **37**, 101630 (2021). doi: 10.1016/j.addma.2020.101630
139. S. A. Khairallah *et al*., Controlling interdependent meso-nanosecond dynamics and defect generation in metal 3D printing. *Science* **368**, 660–665 (2020). doi: 10.1126/science.aay7830; pmid: 32381724
140. R. Cunningham *et al*., Keyhole threshold and morphology in laser melting revealed by ultrahigh-speed x-ray imaging. *Science* **363**, 849–852 (2019). doi: 10.1126/science.aav4687; pmid: 30792298
141. S. A. Khairallah, A. T. Anderson, A. Rubenchik, W. E. King, Laser powder-bed fusion additive manufacturing: Physics of complex melt flow and formation mechanisms of pores, spatter, and denudation zones. *Acta Mater.* **108**, 36–45 (2016). doi: 10.1016/j.actamat.2016.02.014
142. M. Bayat *et al*., Keyhole-induced porosities in Laser-based Powder Bed Fusion (L-PBF) of Ti6Al4V: High-fidelity modelling and experimental validation. *Addit. Manuf.* **30**, 100835 (2019). doi: 10.1016/j.addma.2019.100835
143. T. Keller *et al*., Application of finite element, phase-field, and CALPHAD-based methods to additive manufacturing of Ni-based superalloys. *Acta Mater.* **139**, 244–253 (2017). doi: 10.1016/j.actamat.2017.05.003; pmid: 29230094
144. C. L. Qiu *et al*., On the role of melt flow into the surface structure and porosity development during selective laser melting. *Acta Mater.* **96**, 72–79 (2015). doi: 10.1016/j.actamat.2015.06.004
145. H. Chen, W. T. Yan, Spattering and denudation in laser powder bed fusion process: Multiphase flow modelling. *Acta Mater.* **196**, 154–167 (2020). doi: 10.1016/j.actamat.2020.06.033
146. C. Zhao *et al*., Bulk-explosion-induced metal spattering during laser processing. *Phys. Rev. X* **9**, 021052 (2019). doi: 10.1103/PhysRevX.9.021052
147. N. D. Parab *et al*., Ultrafast X-ray imaging of laser-metal additive manufacturing processes. *J. Synchrotron Radiat.* **25**, 1467–1477 (2018). doi: 10.1107/S1600577518009554; pmid: 30179187
148. C. Zhao *et al*., Real-time monitoring of laser powder bed fusion process using high-speed X-ray imaging and diffraction. *Sci. Rep.* **7**, 3602 (2017). doi: 10.1038/s41598-017-03761-2; pmid: 28620232
149. C. Zhao *et al*., Critical instability at moving keyhole tip generates porosity in laser melting. *Science* **370**, 1080–1086 (2020). doi: 10.1126/science.abd1587; pmid: 33243887
150. I. Todd, No more tears for metal 3D printing. *Nature* **549**, 342–343 (2017). doi: 10.1038/549342a; pmid: 28933429
151. S. M. Thompson, L. K. Bian, N. Shamsaei, A. Yadollahi, An overview of Direct Laser Deposition for additive manufacturing; Part I: Transport phenomena, modeling and diagnostics. *Addit. Manuf.* **8**, 36–62 (2015). doi: 10.1016/j.addma.2015.07.001
152. R. Acharya, J. A. Sharon, A. Staroselsky, Prediction of microstructure in laser powder bed fusion process. *Acta Mater.* **124**, 360–371 (2017). doi: 10.1016/j.actamat.2016.11.018
153. H. Fayazfar *et al*., A critical review of powder-based additive manufacturing of ferrous alloys: Process parameters, microstructure and mechanical properties. *Mater. Des.* **144**, 98–128 (2018). doi: 10.1016/j.matdes.2018.02.018
154. B. AlMangour, D. Grzesiak, J. Q. Cheng, Y. Ertas, Thermal behavior of the molten pool, microstructural evolution, and tribological performance during selective laser melting of TiC/316L stainless steel nanocomposites: Experimental and simulation methods. *J. Mater. Process. Technol.* **257**, 288–301 (2018). doi: 10.1016/j.jmatprotec.2018.01.028
155. A. T. Sidambe, Y. Tian, P. B. Prangnell, P. Fox, Effect of processing parameters on the densification, microstructure and crystallographic texture during the laser powder bed fusion of pure tungsten. *Int. J. Refract. Met. Hard Mater.* **78**, 254–263 (2019). doi: 10.1016/j.ijrmhm.2018.10.004
156. I. Alexander *et al*., Machining of thin-walled parts produced by additive manufacturing technologies. *Procedia CIRP* **41**, 1023–1026 (2016). doi: 10.1016/j.procir.2015.08.088
157. M. P. Sealy, G. Madireddy, R. E. Williams, P. Rao, M. Toursangsaraki, Hybrid processes in additive manufacturing. *Trans. ASME J. Manuf. Sci. Eng.* **140**, 060801 (2018). doi: 10.1115/1.4038644
158. S. Yin *et al*., Hybrid additive manufacture of 316L stainless steel with cold spray and selective laser melting: Microstructure and mechanical properties. *J. Mater. Process. Technol.* **273**, 116248 (2019). doi: 10.1016/j.jmatprotec.2019.05.029
159. N. Kalentics, M. O. V. de Seijas, S. Griffiths, C. Leinenbach, R. E. Logé, 3D laser shock peening—A new method for improving fatigue properties of selective laser melted parts. *Addit. Manuf.* **33**, 101112 (2020). doi: 10.1016/j.addma.2020.101112
160. P. J. Noell, J. M. Rodelas, Z. N. Ghanbari, C. M. Laursen, Microstructural modification of additively manufactured metals by electropulsing. *Addit. Manuf.* **33**, 101128 (2020). doi: 10.1016/j.addma.2020.101128
161. Airbus SE, "Pioneering bionic 3D printing" (2016); www.airbus.com/newsroom/news/en/2016/03/Pioneering-bionic-3D-printing.html.
162. D. Buchbinder, W. Meiners, N. Pirch, K. Wissenbach, J. Schrage, Investigation on reducing distortion by preheating during manufacture of aluminum components using selective laser melting. *J. Laser Appl.* **26**, 012004 (2014). doi: 10.2351/1.4828755
163. N. Shamsaei, A. Yadollahi, L. K. Bian, S. M. Thompson, An overview of Direct Laser Deposition for additive manufacturing; Part II: Mechanical behavior, process parameter optimization and control. *Addit. Manuf.* **8**, 12–35 (2015). doi: 10.1016/j.addma.2015.07.002
164. L. Thijs, K. Kempen, J. P. Kruth, J. Van Humbeeck, Fine-structured aluminium products with controllable texture by selective laser melting of pre-alloyed AlSi10Mg powder. *Acta Mater.* **61**, 1809–1819 (2013). doi: 10.1016/j.actamat.2012.11.052
165. J. Suryawanshi *et al*., Simultaneous enhancements of strength and toughness in an Al-12Si alloy synthesized using selective laser melting. *Acta Mater.* **115**, 285–294 (2016). doi: 10.1016/j.actamat.2016.06.009
166. P. R. Gradl *et al*., "Lightweight thrust chamber assemblies using multi-alloy additive manufacturing and composite overwrap," AIAA Propulsion and Energy Forum, Virtual Event (2020). doi: org/10.2514/6.2020-3787
167. T. Kolb, A. Mahr, F. Huber, J. Tremel, M. Schmidt, Qualification of channels produced by laser powder bed fusion: Analysis of cleaning methods, flow rate and melt pool monitoring data. *Addit. Manuf.* **25**, 430–436 (2019). doi: 10.1016/j.addma.2018.11.026
168. J. Whiting, A. Springer, F. Sciammarella, Real-time acoustic emission monitoring of powder mass flow rate for directed energy deposition. *Addit. Manuf.* **23**, 312–318 (2018). doi: 10.1016/j.addma.2018.08.015; pmid: 30984567
169. R. J. Williams *et al*., In situ thermography for laser powder bed fusion: Effects of layer temperature on porosity, microstructure and mechanical properties. *Addit. Manuf.* **30**, 100880 (2019). doi: 10.1016/j.addma.2019.100880
170. Y. N. Zavalov, A. V. Dubrov, V. D. Dubrov, Optical method of on-line temperature monitoring on the melt surface in laser metal deposition technology. *Proc. SPIE* **11056**, 1105633 (2019). doi: 10.1016/j.addma.2018.11.026
171. M. Mahmoudi, A. A. Ezzat, A. Elwany, Layerwise anomaly detection in laser powder-bed fusion metal additive manufacturing. *Trans. ASME J. Manuf. Sci. Eng.* **141**, 031002 (2019). doi: 10.1115/1.4042108
172. C. Barrett, E. MacDonald, B. Conner, F. Persi, Micron-level layer-wise surface profilometry to detect porosity defects in powder bed fusion of Inconel 718. *JOM* **70**, 1844–1852 (2018). doi: 10.1007/s11837-018-3025-7

Downloaded from https://www.science.org on June 14, 2022

173. P. Charalampous, I. Kostavelis, D. Tzovaras, Non-destructive quality control methods in additive manufacturing: A survey. *Rapid Prototyping J.* **26**, 777–790 (2020). doi: 10.1108/RPJ-08-2019-0224
174. J. J. de Pablo *et al*., New frontiers for the Materials Genome Initiative. *NPJ Comput. Mater.* **5**, 41 (2019). doi: 10.1038/s41524-019-0173-4
175. T. Frenzel, M. Kadic, M. Wegener, Three-dimensional mechanical metamaterials with a twist. *Science* **358**, 1072–1074 (2017). doi: 10.1126/science.aao4640; pmid: 29170236
176. A. Camposeo, L. Persano, M. Farsari, D. Pisignano, Additive manufacturing: Applications and directions in photonics and optoelectronics. *Adv. Opt. Mater.* **7**, 1800419 (2019). doi: 10.1002/adom.201800419; pmid: 30775219
177. W. D. Huang, X. Lin, Research progress in laser solid forming of high-performance metallic components at the State Key Laboratory of Solidification Processing of China. *3D Print. Addit. Manuf.* **1**, 156–165 (2014). doi: 10.1089/3dp.2014.0016
178. E. Abele, M. Kniepkamp, Analysis and optimisation of vertical surface roughness in micro selective laser melting. *Surf. Topogr.* **3**, 034007 (2015). doi: 10.1088/2051-672X/3/3/034007
179. T. Mukherjee, T. DebRoy, A digital twin for rapid qualification of 3D printed metallic components. *Appl. Mater. Today* **14**, 59–65 (2019). doi: 10.1016/j.apmt.2018.11.003
180. A. Majeed *et al*., A big data-driven framework for sustainable and smart additive manufacturing. *Robot. Comput.-Integr. Manuf.* **67**, 102026 (2021). doi: 10.1016/j.rcim.2020.102026
181. J. Singh, J. Mazumder, Evolution of microstructure in laser clad Fe-Cr-Mn-C alloy. *Mater. Sci. Technol.* **2**, 709–713 (1986). doi: 10.1179/mst.1986.2.7.709
182. M. Brandt, D. A. Scott, J. M. Yellup, Fibre optic Nd-YAG laser cladding of preplaced Hastelloy C powder. *Surf. Eng.* **11**, 223–232 (1995). doi: 10.1179/sur.1995.11.3.223
183. S. Nowotny, A. Richter, E. Beyer, "Laser cladding using high-power diode lasers," in *Proceedings of the Laser Materials Processing Conference ICALEO'98* (1998), vol. 2, pp. G68–G74. doi: 10.2351/1.5059205
184. J. Mazumder, D. Dutta, N. Kikuchi, A. Ghosh, Closed loop direct metal deposition: Art to part. *Opt. Lasers Eng.* **34**, 397–414 (2000). doi: 10.1016/S0143-8166(00)00072-5
185. T. Wang, Y. Y. Zhu, S. Q. Zhang, H. B. Tang, H. M. Wang, Grain morphology evolution behavior of titanium alloy components during laser melting deposition additive manufacturing. *J. Alloys Compd.* **632**, 505–513 (2015). doi: 10.1016/j.jallcom.2015.01.256
186. J. Witzel, thesis, RWTH Aachen University (2015).
187. B. E. Carroll, T. A. Palmer, A. M. Beese, Anisotropic tensile behavior of Ti-6Al-4V components fabricated with directed energy deposition additive manufacturing. *Acta Mater.* **87**, 309–320 (2015). doi: 10.1016/j.actamat.2014.12.054
188. Q. Liu *et al*., TC17 titanium alloy laser melting deposition repair process and properties. *Opt. Laser Technol.* **82**, 1–9 (2016). doi: 10.1016/j.optlastec.2016.02.013
189. R. Brockmann, A. Candel-Ruiz, S. Kaufmann, O. Müllerschön, "Strategies for high deposition rate additive manufacturing by laser metal deposition," in *ICALEO* (2015), pp. 680–683. doi: 10.2351/1.5063214
190. W. L. Weiss, D. L. Bourell, Selective laser sintering of intermetallics. *Metall. Trans. A* **24**, 757–759 (1993). doi: 10.1007/BF02656644
191. W. Meiners, K. Wissenbach, A. Gasser, "Selective laser sintering at melting temperature," U.S. Patent 6,215,093 B1 (1997).
192. A. K. Nath, in *Laser-Assisted Fabrication of Materials*, J. D. Majumdar, I. Manna, Eds. (Springer, 2013), chap. 2.
193. L. Li, in *Advances in Laser Materials Processing*, J. Lawrence, Ed. (Elsevier, 2018), chap. 2.
194. D. Buchbinder, H. Schleifenbaum, S. Heidrich, W. Meiners, J. Bültmann, High power selective laser melting (HP SLM) of aluminum parts. *Phys. Procedia* **12**, 271–278 (2011). doi: 10.1016/j.phpro.2011.03.035
195. D. D. Gu *et al*., Densification behavior, microstructure evolution, and wear performance of selective laser melting processed commercially pure titanium. *Acta Mater.* **60**, 3849–3860 (2012). doi: 10.1016/j.actamat.2012.04.006
196. P. Wagenblast, A. Myrell, M. Thielmann, T. Scherbaum, D. Coupek, Additive manufacturing with green disk lasers. *Proc. SPIE* **11271**, 112710J (2020). doi: 10.1016/j.phpro.2011.03.035
197. G. Schieber *et al*., in *Modelling Behaviour*, M. R. Thomsen *et al*., Eds. (Springer, 2015), pp. 237–245.
198. H. Yao *et al*., Protection mechanisms of the iron-plated armor of a deep-sea hydrothermal vent gastropod. *Proc. Natl. Acad. Sci. U.S.A.* **107**, 987–992 (2010). doi: 10.1073/pnas.0912988107; pmid: 20133823
199. R. Wang *et al*., Formation mechanisms of TiB_2 tracks on Ti6Al4V alloy during selective laser melting of ceramic-metal multi-material. *Powder Technol.* **367**, 597–607 (2020). doi: 10.1016/j.powtec.2020.04.027
200. K. J. Lin *et al*., Laser powder bed fusion of bio-inspired honeycomb structures: Effect of twist angle on compressive behaviors. *Thin-Walled Struct.* **159**, 107252 (2021). doi: 10.1016/j.tws.2020.107252

ACKNOWLEDGMENTS

We thank three anonymous reviewers for their insightful comments. **Funding:** Supported by National Natural Science Foundation of China grant 51735005, National Key Research and Development Program of China grants 2016YFB1100101 and 2019YFE0107000, National Natural Science Foundation of China for Creative Research Groups grant 51921003, the National High-level Personnel of Special Support Program of China, the Cheung Kong Young Scholars Program of Ministry of Education of China, the Top-Notch Young Talents Program of China, and the Fraunhofer-Bessel Research Award from Alexander von Humboldt Foundation Germany (D.G.); NSFC-DFG Sino-German Research Project grant GZ 1217 (D.G. and R.P.); National Natural Science Foundation of China grant 51790171 (J.Z.); and ASTUTE 2020/ASTUTE EAST (Program for Advanced Sustainable Manufacturing Technologies in Wales), which has been partly funded by the European Regional Development Fund through the Welsh Government (R.S.). **Author contributions:** D.G. conceived and wrote the article; R.P., D.L.B., R.S., and J.Z. discussed and edited its contents; D.G., J.Z., and X.S. conceptualized and prepared the planetary exploration lander example. **Competing interests:** The authors declare no competing interests.

10.1126/science.abg1487

Downloaded from https://www.science.org on June 14, 2022

Science

Material-structure-performance integrated laser-metal additive manufacturing

Dongdong GuXinyu ShiReinhart PopraweDavid L. BourellRossitza SetchiJihong Zhu

Science, 372 (6545), eabg1487. • DOI: 10.1126/science.abg1487

Cross-scale coordination

Laser-based additive manufacturing has the potential to revolutionize how components are designed. Gu *et al.* suggest moving away from a strategy that designs and builds components in a serial manner for a more wholistic method of optimization for metal parts. The authors summarize several key developments in laser powder bed fusion and directed energy deposition and outline a number of issues that still need to be overcome. A more integrated approach will help to reduce the number of steps required for fabrication and expand the types of structures available for end-use components.

Science, abg1487, this issue p. eabg1487

View the article online
https://www.science.org/doi/10.1126/science.abg1487
Permissions
https://www.science.org/help/reprints-and-permissions

Downloaded from https://www.science.org on June 14, 2022

Use of this article is subject to the Terms of service

Science (ISSN 1095-9203) is published by the American Association for the Advancement of Science. 1200 New York Avenue NW, Washington, DC 20005. The title *Science* is a registered trademark of AAAS.
Copyright © 2021 The Authors, some rights reserved; exclusive licensee American Association for the Advancement of Science. No claim to original U.S. Government Works